H
APPENDIX
CEUS SSC MODEL HAZARD INPUT DOCUMENT (HID)

H.1 Introduction

This appendix describes the CEUS SSC Model in the main report. The purpose of this document is to provide the necessary information so that an analyst experienced in PSHA can implement the seismic source model. The appendix contains the logic tree structure and descriptions of the parameters that define the frequency and spatial distribution of potential future earthquakes. The reader is referred to the main report for detailed descriptions of methods and rationale used to develop the model parameters. The digital files that contain the input parameters described in this appendix are contained on the project website. The area covered by this model is shown on Figure H-1-1 along with the locations of the test sites used for hazard sensitivity calculations presented in Chapter 8.

H.2 Seismic Source Model Structure and Master Logic Tree

The structure of the CEUS SSC model is described in Section 4. The CEUS SSC Model contains two general types of seismic sources. The first type of seismic source uses the recorded history of seismicity to model the frequency and spatial distribution of moderate to large earthquakes ($\mathbf{M} \geq 5$). These sources are denoted as distributed seismicity sources. They cover the entire region shown on Figure H-1-1. The second type of seismic source uses the paleo-earthquake record to model the frequency and spatial distribution of repeated large magnitude earthquakes (RLMEs) at specific locations.

Figure H-2-1 shows the master logic tree for the CEUS SSC model. The basis for this logic tree is described in Section 4.2. The first node addresses the conceptual approach used to characterize the distributed seismicity sources. Two approaches are used. The first is an approach in which distributed seismicity is modeled using seismicity rates that smoothly vary across the entire study region. The study region is subdivided only on the basis of differences in maximum magnitudes. The first branch is designated as the Mmax Zones approach. The second approach uses seismic source zones defined on a seismotectonic basis to model distributed seismicity. The second branch is designated as the Seismotectonic Zones approach. In both approaches specific seismic sources are used to model individual sources of RLMEs. The RLME sources represent additional sources of seismic hazard that are added to the hazard from the distributed seismicity sources.

The models developed for the various types of seismic sources are described in subsequent sections of this appendix.

H.3 Mmax Zones Distributed Seismicity Sources

Figure H-3-1 shows the logic tree structure to be used for the distributed seismicity sources on the Mmax Zones branch of the master logic tree. This logic tree is discussed in Section 4.2.3 of the main report.

H.3.1 Division of Study Region

The first node addresses whether or not the study region is divided into two zones that have different Mmax distributions. If "No" then the entire study region, shown on Figure H-1-1, is treated as a single source. If "Yes" then the study region is divided into Mesozoic and younger extended regions (MESE) and those regions that do not display such evidence (NMESE).

H.3.2 Location of Boundary of Mesozoic Extension

The second node of the Mmax Zones logic tree, which applies only to the Mesozoic and younger separation branch, addresses the alternative boundaries between the MESE and NMSES regions. Two alternatives are used. The first, labeled the "Wide Interpretation" has a broad interpretation of the extent of Mesozoic extension. Figure H-3-2 shows the location of this boundary. The second, labeled the "Narrow Interpretation" makes a narrow interpretation of the extent of Mesozoic extension. Figure H3-3 shows the location of this boundary.

H.3.3 Magnitude Interval Weights for Fitting Earthquake Occurrence Parameters

The third node addresses the issue of the weight assigned to smaller magnitudes in the estimation of seismicity parameters for the seismic source zones. Three cases are used, Cases A, B, and E. The weights assigned to individual magnitude intervals are discussed in Section 5.3.2.2.

H.3.4 Mmax Zones

The next element of the Mmax Zones logic tree (which is not a node but a listing) identifies the Mmax zone designations for each case. The vertical bar without a dot at the branching point designates the addition of hazard from all of the listed sources, as opposed to weighted alternatives that appear with a dot on the logic tree. The coordinates defining the boundaries of the Mmax Zones are contained in the file Source_Zones_Geometry.zip on the project web site. The boundary for each zone is contained in an ASCII file named for the source with the extension "zon" (e.g. "MESE-N.zon" for the MESE-N Mmax zone).

H.3.5 Seismogenic Crustal Thickness

The fifth node of the logic tree represents the uncertainty distribution for seismogenic crustal thickness. The distribution used for each Mmax zone is listed in Table H-3-1. These are epistemic uncertainties representing weighted alternative assessments of the seismogenic crustal thickness for each Mmax zone.

H.3.6 Future Earthquake Rupture Characteristics

The sixth node addresses the uncertainty distributions for the rupture characteristics of future earthquakes. In the CEUS SSC model a single aleatory distribution is applied to each Mmax zone. These aleatory distributions are listed in Table H-3-2.

The area of individual earthquake ruptures is modeled using the relationship:

$$\log_{10}(\text{A in km}^2) = \mathbf{M} - 4.366 \qquad \text{(H-1)}$$

The rupture aspect ratio is 1:1 until the rupture reaches maximum rupture width. For larger ruptures the width is fixed and the length is increased to obtain the area given by Equation H-1. This model is used for all earthquake sources described in this HID.

H.3.7 Assessment of Seismicity Rates

The seventh node of the Mmax Zones logic tree on Figure H-3-1 addresses the approach used for assessing seismicity rates and their spatial distribution. Allowing both the *a*-value and the *b*-value to vary spatially is the selected approach. The approach is described in Section 5.3.2. Seismicity parameters are estimated for ½° longitude by ½° latitude cells or partial cells.

H.3.8 Degree of Smoothing Applied in Defining Spatial Smoothing of Seismicity Rates

The eighth node of the logic tree addresses the degree of smoothing applied in the seismicity parameter estimation in each source region. A single approach, the "Objective" approach, is used to select the degree of smoothing. This is discussed in Section 5.3.2.2 of the main report.

H.3.9 Uncertainty in Earthquake Recurrence Rates

The ninth node of the logic tree addresses the epistemic uncertainty in earthquake recurrence parameters. The recurrence parameter distributions are represented by eight alternative spatial distributions developed from the fitted parameter distributions. These alternatives are described in Section 5.3.2. The result is eight equally weighted alternative sets of recurrence parameters for each Mmax Zone. The recurrence parameters are contained in the file "CEUS_SSC_All_xyab_Files.zip" on the project web site. The recurrence parameters are contained in ASCII files for each Mmax zone using the following file naming convention.

Zone_Case_Realization.ext

The *"Zone*" portion of the file name is the Mmax Zone name, MESE-W, MESE-N, NMESE-W, NMESE-N, and STUDY_R for the case when the entire study region is considered a single Mmax Zone. The "*Case*" portion of the file name refers to Case A, Case B, or Case E on Figure H-4. The "*Realization*" portion of the file name takes on the values "01", "02", "03", "04", "05", "06", "07", and "08" to indicate the eight equally weighted alternative sets of recurrence parameters. The "*ext*" portion of the file name takes on two values. An extension of "*xyab*" indicates a file containing recurrence parameters for PSHA calculations that integrate over magnitude starting from a minimum magnitude, m_0, of **M** 5.0. An extension of "*xyab4*" indicates a file containing recurrence parameters for PSHA calculations that integrate over magnitude starting from a minimum magnitude, m_0, of **M** 4.0, which would typically be used for PSHA calculations incorporating the Cumulative Absolute Velocity (CAV) filter.

Each recurrence parameter file contains a header with the case description. The second record provides the number of individual cells and the nominal cell size in degrees (e.g 0.5 for ½° longitude by ½° latitude cells). The remaining records contain the following information in five columns:

- Longitude and latitude of the center of the cell or partial cell, in degrees.
- Recurrence rate of earthquakes of magnitude m_0 and larger per equatorial degrees^2. For the files with extension "*xyab*" this is the rate of **M** 5 and larger earthquakes and for files with extension "*xyab4*" this is the rate of **M** 4 and larger earthquakes.
- Beta value. This is the *b*-value expressed in natural log units $\{\beta = b \times \ln(10)\}$.
- Area of the cell in equatorial degrees^2. The absolute value of recurrence rate is the product of the values in the third and fifth columns.

H.3.10 Uncertainty in Maximum Magnitude

The tenth node of the logic tree addresses the uncertainty in the maximum magnitude for each Mmax Zone. These epistemic distributions are listed in Table H-3-3.

H.4 Seismotectonic Zones

Figure H-4-1 shows the logic tree structure for the seismotectonic source zones component of the master logic tree. The components of the source model logic tree are described below. Table H-4-1 lists the seismotectonic source zones.

H.4.1 Alternative Zonation Models

The first two nodes address the alternative zonation models. The first node addresses the uncertainty in the western boundary of the Paleozoic Extended Crust seismotectonic zone. The two alternatives are the narrow interpretation (0.8) and the wide interpretation (0.2). The second node of the logic tree addresses the uncertainty in the eastern extent of the Reelfoot Rift zone (RR) —whether or not it includes the Rough Creek Graben (RCG). These two logic tree levels lead to the four alternative seismotectonic zonation configurations shown on Figures H-4-2 through H-4-5. The discussion of this assessment and the associated weights is given in Section 7.3.6.3 of the main report. As shown on Figures H-4-1 though H-4-5, the alternative zonation models produce alternative versions of the Mid-Continent source zone. These are designated MidC-A, MidC-B, MidC-C, and MidC-D.

H.4.2 Magnitude Interval Weights for Fitting Earthquake Occurrence Parameters

The third node addresses the issue of the weight assigned to smaller magnitudes in the estimation of seismicity parameters for the seismic source zones. As in the Mmax Zones model, three cases are used, Cases A, B, and E. The weights assigned to individual magnitude intervals are discussed in Section 5.3.2.2.

H.4.3 Seismotectonic Zones

The next element of the logic tree is again a listing of the individual seismotectonic source zones for each zonation model. The vertical bar without a dot at the branching point designates the addition of hazard from all of the listed sources. The coordinates defining the boundaries of the source are contained in the file Source_Zones_Geometry.zip on the project web site. The boundary for each zone is contained in an ASCII file named for the source with the extension "zon" (e.g. "AHEX.zon" for the AHEX seismotectonic source zone).

H.4.4 Seismogenic Crustal Thickness

The fifth node of the logic tree represents the uncertainty distribution for seismogenic crustal thickness. The distribution used for each seismotectonic zone is listed in Table H-4-2. These are epistemic uncertainties representing weighted alternatives.

H.4.5 Future Earthquake Rupture Characteristics

The sixth node addresses the uncertainty distributions for the rupture characteristics of future earthquakes. In the CEUS SSC model a single aleatory distribution is applied to each seismotectonic zone. These aleatory distributions are listed in Table H-4-3.

The area of individual earthquake ruptures is modeled using the relationship given in Equation H-1 above. The rupture aspect ratio is 1:1 until the rupture reaches maximum rupture width. For larger ruptures the width is fixed and the length is increased to obtain the area given by Equation H-1. This model is used for all earthquake sources described in this HID.

H.4.6 Assessment of Seismicity Rates

The seventh node of the logic tree on Figure H-4-1 addresses the approach used for assessing seismicity rates and their spatial distribution. Allowing both the *a*-value and the *b*-value to vary spatially is the selected approach. The approach is described in Section 5.3.2. Seismicity parameters are estimated for ¼° longitude by ¼° latitude cells or partial cells for all sources except the Mid-Continent sources, for which the cell size ½° longitude by ½° latitude is used.

H.4.7 Degree of Smoothing Applied in Defining Spatial Smoothing of Seismicity Rates

The eighth node of the logic tree addresses the degree of smoothing applied in the seismicity parameter estimation in each source region. A single approach is used to select the degree of smoothing for each source. This is discussed in Section 5.3.2.2 of the main report. For all sources but the St. Lawrence Rift zone (SLR) the "Objective" approach is used.

H.4.8 Uncertainty in Earthquake Recurrence Rates

The ninth node of the logic tree addresses the epistemic uncertainty in earthquake recurrence parameters. As was the case for the Mmax zones, the recurrence parameter distributions are represented by eight alternative spatial distributions developed from the fitted parameter distributions. These alternatives are described in Section 5.3.2. The result is eight equally weighted alternative sets of recurrence parameters for each Seismotectonic Zone. The recurrence parameters are contained in the file "CEUS_SSC_All_xyab_Files.zip" on the project web site. The recurrence parameters are contained in ASCII files for each seismotectonic zone using the naming convention and file format described in Section H.3.9.

H.4.9 Uncertainty in Maximum Magnitude

The tenth node of the logic tree addresses the uncertainty in the maximum magnitude for each seismotectonic zone. These distributions are listed in Table H-4-4.

H.5 RLME Sources

This section describes the models for the RLME sources. As shown on Figure H-2-1, these sources are considered to be additional sources superimposed on the distributed seismicity sources on the seismotectonic branch of the master logic tree or on the Mmax Zones on the Mmax Zone branch of the master logic tree. Figure H-5-1 shows the overall structure of the RLME sources model. There are 10 RLME sources. Each source has a logic tree defining the uncertainty in characterization. Discussion of the each of the individual RLME sources is contained in Section H.5 of the main report. The locations of the RLME sources are shown on Figure H-5-2. The parameters for each of the RLME sources present in the following sections are contained in files located on the CEUS SSC Project website in the RLME directory.

H.5.1 Charlevoix RLME Seismic Source Model

The Charlevoix RLME source is described in Section 6.1.1 of the main text. The logic tree for the Charlevoix RLME source is shown on Figure H-5.1-1. The parameters are located on the CEUS SSC Project web site in the file "Charlevoix_RLME.xls."

H.5.1.1 Temporal Clustering

The first node of the logic tree addresses the issue of temporal clustering of earthquakes in the present tectonic stress regime. This node of the logic tree is not applicable to the Charlevoix RLME source.

H.5.1.2 Localizing Tectonic Features

Because the occurrence of RLMEs in the Charlevoix zone cannot be associated with a specific feature, future RLMEs are modeled as occurring randomly within the RLME source zone, as indicated on the second node of the logic tree (Figure H-5.1-1).

H.5.1.3 Geometry and Style of Faulting

The geometry of the Charlevoix RLME source is shown on Figure H-5.1-2. A single source zone geometry is used. The coordinates are contained on the "Geometry" tab of the file "Charlevoix_RLME.xls." Given the small source size and uncertain fault locations, the boundaries of the Charlevoix RLME source are leaky, allowing ruptures to extend beyond the source boundary by 50 percent.

The thickness of seismogenic crust is modeled with equal weight on 25 and 30 km (16 and 19 mi.), as shown on the fourth node of the logic tree (Figure H-5.1-1).

Future earthquake ruptures are modeled as reverse faulting earthquakes. Rupture geometry is modeled by a single aleatory distribution as shown by the fifth node of the logic tree. Strikes of ruptures are to be uniformly distributed over azimuths of 0 to 360 degrees. Fault dips are uniformly distributed between 45 and 60 degrees.

H.5.1.4 RLME Magnitude

Table H-5.1-1 lists the epistemic uncertainty distribution for the expected magnitude of future earthquakes associated with the Charlevoix RLME source. Aleatory variability in the size of an individual Charlevoix RLME is modeled as a uniform distribution of ±0.25 **M** units centered on the expected RLME magnitude value listed in Table H-5.1-1.

H.5.1.5 RLME Recurrence

The remaining nodes of the Charlevoix RLME logic tree address uncertainties in the specification of the annual frequency of RLMEs.

Recurrence Methods and Data

Two approaches are used to assess RLME recurrence. The “Earthquake Recurrence Intervals” approach is assigned a weight of 0.2. This approach leads to data set 1. The “Earthquake Count in a Time Interval” approach is assigned a weight of 0.8. There are two data sets associated with this branch. Data set 2 is assigned a conditional weight of 0.75 and data set 3 is assigned a conditional weight of 0.25.

Earthquake Recurrence Model

The Poisson model is used as the earthquake recurrence model, with a weight of 1.0.

RLME Annual Frequency

The final node of the logic tree addresses the uncertainty distributions for the annual frequency of RLMEs. These distributions are listed in Tables H-5.1-2, H-5.1-3, and H-5.1-4. The data are contained in the file “Charlevoix_RLME.xls.”

H.5.2 Charleston RLME Seismic Source Model

Charleston RLME source is described in Section 6.1.2 of the main text. Figure H-5.2-1 shows the logic tree for the Charleston RLME source. The parameters are located on the CEUS SSC Project web site in the file “Charleston_RLME.xls.”

H.5.2.1 Temporal Clustering

The first node of the logic tree (Figure H-5.2-1) addresses the issue of temporal clustering of earthquakes on the Charleston RLME source. The Charleston RLME seismic source is modeled as “in” a temporal cluster with a weight of 0.9 and “out” of a temporal cluster with a weight of 0.1. For the “in” branch, the remaining portion of the logic tree is used to define the hazard from this source. On the “out” branch the Charleston RLME source is not included in calculation of the total seismic hazard.

H.5.2.2 Localizing Feature

The second node of the Charleston RLME source logic tree indicates whether future earthquakes in the Charleston seismic zone will be associated with a specific localizing tectonic feature. The approach used for this source is to model future ruptures to occur randomly with the source.

H.5.2.3 Geometry and Style of Faulting

The third node of the Charleston RLME source logic tree addresses the alternative geometries of the parameters Charleston RLME source. Three alternative source zone geometries are included in the model. These are shown on Figure H-5.2-2. The coordinates of the three source geometries are given in the file "Charleston_RLME.xls."

The fourth node of the logic tree indicates the three values of seismogenic crustal thickness used for all source geometries.

The geometries and style of faulting for the three source geometries are specified as follows.

- Charleston Local source configuration: Future ruptures are oriented northeast, parallel to the long axis of the zone. Ruptures are modeled as occurring on vertical strike-slip faults. All boundaries of the Charleston Local source are strict, such that ruptures are not allowed to extend beyond the zone boundaries.
- Charleston Narrow source configuration: Future ruptures are oriented north-northeast, parallel to the long axis of the zone. Ruptures are modeled as occurring on vertical strike-slip faults. The northeast and southwest boundaries of the Charleston Narrow source are leaky, whereas the northwest and southeast boundaries of the Charleston Narrow source are strict.
- Charleston Regional source configuration: Future rupture orientations are represented by two alternatives: (1) future ruptures oriented parallel to the long axis of the source (northeast) with 0.80 weight, and (2) future ruptures oriented parallel to the short axis of the source (northwest) with 0.20 weight. In both cases, future ruptures are modeled as occurring on vertical strike-slip faults. All boundaries of the Charleston Regional source are strict.

H.5.2.4 RLME Magnitude

The sixth node of the Charleston RLME source logic tree defines the magnitude of future large earthquakes in the Charleston RLME source. The RLME magnitude distribution is given in Table H-5.2-1. Aleatory variability in the size of an individual Charleston RLME is modeled as a uniform distribution of ±0.25 **M** units centered on the expected RLME magnitude value.

H.5.2.5 RLME Recurrence

The remaining nodes of the Charleston RLME source logic tree address the uncertainty in modeling of the recurrence rare of Charleston RLMEs.

Recurrence Method

The recurrence data for the Charleston RLME source consists of ages of past RLMEs estimated from the paleoliquefaction record. Therefore, node seven of the logic tree indicates that recurrence for the Charleston RLME source is based solely on the "Earthquake Recurrence Intervals" approach.

Time Period

The eighth node of the Charleston RLME source logic tree assesses length and completeness of the paleoliquefaction record. Two alternatives are considered: the approximately 2,000-year record of Charleston earthquakes with 0.80 weight and the approximately 5,500-year record with 0.20 weight.

Earthquake Count

The ninth node of the Charleston logic tree addresses the uncertainty in the number of RLMEs that have occurred in the Charleston RLME source. For the 2,000-year record, a single model is used. For the 5.500-year, three alternatives are used as shown on Figure H-5.2-1.

Earthquake Recurrence Model

The tenth node of the Charleston RLME source logic tree defines the earthquake recurrence models used for the regional, local, and narrow source zones (Figure H-5.2-1). For the regional and local sources, only the Poisson model is used. For the more "fault-like" narrow source zone, the Poisson model is assigned 0.90 weight, and the BPT renewal model is assigned 0.10 weight. Use of the BPT renewal model requires specification of the coefficient of variation of the repeat time for RLMEs, parameter α. The uncertainty distribution for α is shown on the eleventh node of the Charleston RLME source logic tree.

RLME Annual Frequency

The final (twelfth) node of the logic tree addresses the uncertainty distributions for the annual frequency of RLMEs. There are 20 uncertainty distributions corresponding to the various approaches and data sets defined in Levels 8, 9, 10, and 11 of the logic tree. These are given in Tables H-5.2 -2 through H-5.2-21. Tables H-5.2-2 through H-5.2-6 provide the recurrence rate distributions for the Poisson Occurrence model and Tables H-5.2-7 through H-5.2-21 provide the recurrence rate distributions for the BPT Renewal model. Figure H-5.2-1 shows the relationship between the branches of the logic tree and the recurrence rate distribution tables.

H.5.3 Cheraw RLME Seismic Source Model

The Cheraw RLME source is described in Section 6.1.3 of the main report. Figure H-5.3-1 shows the logic tree for the Cheraw RLME source. The parameters are located on the CEUS SSC Project web site in the file "Cheraw_RLME.xls."

H.5.3.1 Temporal Clustering

The first node of the logic tree (Figure H-5.3-1) addresses the issue of temporal clustering of earthquakes in the present tectonic stress regime. The within-cluster branch of the logic tree is assigned a weight of 0.9, and the out-of-cluster branch is assigned a weight of 0.1. These two branches lead to different recurrence rates

H.5.3.2 Localizing Feature

The Cheraw RLME source is modeled as a single fault source.

H.5.3.3 Geometry and Style of Faulting

Two alternative lengths are used for the Cheraw RLME source. These are shown on Figure H-5.3-2. The mapped length is assigned a weight of 0.8 and the extended length is assigned a weight of 0.2. The coordinates for these two geometries are provided in the file "Cheraw_RLME.xls."

The fourth node of the logic tree provides the uncertainty distribution for the thickness of seismogenic crust. The generic distribution of 13 km (weight of 0.4), 17 km (weight of 0.4), and 22 km (weight of 0.2) is used.

The fifth node of the logic tree addresses the uncertainty in the dip of the fault. The assigned uncertainty distribution is: 50°NW (0.6), 65°NW (0.4).

The style of faulting is assessed to be normal. Future ruptures are to be confined to the modeled fault surface.

H.5.3.4 RLME Magnitude

The magnitude distribution for the Cheraw RLME source is given in Table H-5.3-1. Aleatory variability in the size of an individual Cheraw RLME is modeled as a uniform distribution of ±0.25 **M** units centered on the expected RLME magnitude value.

H.5.3.5 RLME Recurrence

The remaining nodes of the Cheraw RLME logic tree address the uncertainties in modeling the recurrence rate of Cheraw RLMEs

Recurrence Method

Two types of data are used for assessing the recurrence frequency of Cheraw RLMEs. The first is the average slip rate of the fault and the second is the number and timing of previous RLMEs, allowing application of the "Earthquake Recurrence Intervals" approach. These two approaches are assigned equal weights.

Recurrence Data

Two data sets are used for the assessment of the in-cluster recurrence rate of Cheraw RLMEs based on the "Earthquake Recurrence Intervals" approach. The first is the occurrence of two earthquakes in 20-25 ka, with a weight of 0.4, and the second in the occurrence of three earthquakes in 20-25 ka, with a weight of 0.6. The total slip of the fault in the range of 3.2 to 4.1 m in 20-25 ka is used to assess the in-cluster slip rate.

The out-of-cluster recurrence rates for the "Earthquake Recurrence Intervals" approach are based on estimates of the time between in-cluster periods. Out-of-cluster slip rate is based on 7–8 m of offset in a time period ranging from 400 ka to 2 Ma.

Earthquake Recurrence Model

The Poisson model is used as the earthquake recurrence model with weight 1.0 for the Cheraw RLME source.

RLME Annual Frequency

The assessed RLME recurrence frequencies for the various data sets are given in Tables H-5.3-2 through H-5.3-6. Figure H-5.3-1 shows the relationship between the branches of the logic tree and the recurrence rate distribution tables.

H.5.4 Meers RLME Seismic Source Model

The Meers RLME source is described in Section 6.1.4 of the main report. The source logic tree is shown on Figure H-5.4-1. The data for the Meers RLME is located on the CEUS SSC Project web site contained in file “Meers_RLME.xls.”

H.5.4.1 Temporal Clustering

The first node of the logic tree (Figure H-5.4-1) addresses the issue of temporal clustering. The in-cluster branch of the logic tree is given a weight of 0.8 and the out-of-cluster branch a weight of 0.2. These two alternatives affect both the recurrence rate of the RLMEs and their spatial distribution.

H.5.4.2 Localizing Feature

The second branch of the logic tree (Figure H-5.4-1) defined whether future earthquakes associated with the Meers RLME source are localized along the Meers fault scarp (designated “Fault” on the logic tree), or whether they may occur along other structures within the Oklahoma aulacogen (“Random in Zone” on the logic tree). For the in-cluster case, the “Fault” model is used and RLMEs are constrained to occur on the Meers fault. For the out-of-cluster case, RLMEs the two alternatives are the “Fault” model and the “Random in Zone” model.

H.5.4.3 Geometry and Style of Faulting

The third through fifth branches of the logic tree describe the source geometry and style of faulting (Figure H-5.4-1).

The alternative geometries for the “Fault” model consists of the mapped Quaternary trace of the Meers fault (weight 0.9) and an extended fault trace (weight 0.1). These two geometries are shown on Figure H-5.4-2.

For the “Random-in-Zone” model, the RLMEs are modeled as occurring uniformly distributed within the boundary of the OKA seismic source zone, also shown on Figure H-5.4-2.

The seismogenic thickness for the Meers RLME source is modeled as either 15 km or 20 km with equal weights.

For the “Fault” model, future earthquake ruptures are to be modeled as either oblique earthquakes on a vertical fault (weight 0.5) or reverse-oblique earthquakes dipping 40 degrees southwest. Ruptures are confined to the model fault surface.

For the "Random-in-Zone" model future ruptures are to be modeled as having a N60W strike and a random dip in the range of 90 to 40 degrees southwest.

H.5.4.4 RLME Magnitude

The sixth branch of the logic tree describes the earthquake magnitudes for the Meers RLME. The RLME magnitude distribution is given in Table H-5.4-1. Aleatory variability in the size of an individual Meers RLME is modeled as a uniform distribution of ±0.25 **M** units centered on the expected RLME magnitude value.

H.5.4.5 RLME Recurrence

The remaining branches of the logic tree define the uncertainty distributions for RLME recurrence rates.

Recurrence Method

The "Earthquake Recurrence Intervals" approach is used with weight 1.0 (Figure H-5.4-1).

Recurrence Data

The data used to assess the in-cluster recurrence rates consists of two earthquakes in 2.1 to 3 ka. The data used to assess the out-of-cluster case consist of the estimated time between clusters of activity on the fault.

Earthquake Recurrence Model

The Poisson model is used as the earthquake recurrence model with weight 1.0 for the Meers RLME source.

RLME Annual Frequency

The final node of the logic tree addresses the uncertainty distributions for the annual frequency of RLMEs (Figure H-5.4-1). These distributions are provided in Tables H-5.4-2 for the in-cluster case and Table H-5.4-3 for the out-of-cluster case. Note that the out-of-cluster model combined with the "Random-in-Zone" model for the spatial distribution is assigned the in-cluster recurrence rate distribution.

H.5.5 New Madrid Fault System RLME Seismic Source Model

The New Madrid Fault System (NMFS) RLME is discussed in Section 6.1.5 of the main report. Figure H-5.5-1 shows the logic tree for this source. The data for this source is on the CEUS SSC Project web site contained in file "NMFS_RLME.xls."

H.5.5.1 Temporal Clustering

The first node of the logic tree (Figure H-5.5-1) addresses the issue of temporal clustering. Three alternatives are modeled.

- With weight 0.9 the NMFS RLME is modeled as being in-cluster.

- With weight 0.05 the RLME is modeled as being out-of-cluster with no earthquake activity occurring on the source.
- With weight 0.05, the RLME is modeled as being out-of-cluster with a long term rate assigned to only the Reelfoot Thrust (described below).

H.5.5.2 Localizing Feature

The RLMEs associated with the NMFS are modeled as occurring on three fault sources: (1) the New Madrid South (NMS) fault; (2) the New Madrid North (NMN) fault; and (3) the Reelfoot Thrust (RFT).

H.5.5.3 Geometry and Style of Faulting

Each of the NMFS fault sources has two alternative geometries as shown on Figures H-5.5-2, H-5.5-3, and H-5.5-4, respectively. Future NMFS RLMEs are confined to occur on these modeled faults.

The seismogenic crustal thickness is modeled as being 13 km (weight of 0.3), 15 km (weight of 0.5), or 17 km (weight of 0.2).

The style of faulting for each of the fault sources is based on geologic and seismologic observations. The NMS fault is modeled as a vertical right-lateral strike-slip fault. The RFT fault is modeled as a reverse fault dipping an average of 40 degrees southwest. The NMN fault is modeled as a vertical right-lateral strike-slip fault.

H.5.5.4 RLME Magnitude

The magnitudes of RLMEs for the NMFS are assigned in terms of a joint distribution. Table H-5.5-1 lists the assigned distribution of rupture sets. Aleatory variability in the size of an individual RLME is modeled as a uniform distribution of ±0.25 **M** units centered on the expected RLME magnitude value for each fault source.

H.5.5.5 RLME Recurrence

The remaining nodes of the NMFS RLME source logic tree address the assessment of earthquake recurrence rates.

Recurrence Method

The "Earthquake Recurrence Intervals" approach is used with weight 1.0 (Figure H-5.5-1).

Recurrence Data

In-cluster case recurrence rates are based on the 1811-1812, 1450 AD, and 900 AD sequences. Out-of-cluster recurrence rates for the NMFS are based on timing between clusters.

Earthquake Recurrence Model

The Poisson and renewal recurrence models are assigned weights of 0.75 and 0.25, respectively, for the in-cluster case. For the renewal model the BPT model is used with a distribution for the parameter α shown on the twelfth node of the source logic tree.

RLME Annual Frequency

The final node of the logic tree addresses the uncertainty distributions for the annual frequency of RLMEs (Figure H-5.5-1). These distributions are contained in Table H-5.5-2 for the in-cluster Poisson case, Tables H-5.5-3, H-5.5-4, and H-5.5-5 for the in-cluster renewal model cases, and in Table H-5.5-5 for the out-of-cluster Poisson case.

For the in-cluster case, RLMEs are to be modeled as occurring on all three of the fault sources within a close period of time (e.g. similar to the 1811-1812 earthquake sequence).

H.5.6 Eastern Rift Margin Fault RLME Seismic Source Model

The Eastern Rift Margin (ERM) fault RLME sources are described in Section 6.1.6 in the main text. The source consists of southern and northern segments. Figure H-5.6-1 shows the logic tree for the southern segment, ERM-S and Figure H-5.6-2 shows the logic tree for the northern segment ERM-N. The data for these two sources are contained on the CEUS SSC Project web site in files “ERM-S_RLME.xls” and “ERM-N_RLME.xls.”

H.5.6.1 Temporal Clustering

The first node of the logic trees addresses the issue of temporal clustering of earthquakes in the present tectonic stress regime. This node of the logic tree is not applicable to the ERM-S and ERM-N RLME sources.

H.5.6.2 Localizing Feature

The ERM-S and ERM-N RLME sources are modeled as narrow zones. Figures H-5.6-3 and H-5.6-4 show the geometries of the sources. Earthquakes are modeled as uniformly distributed in the source zones.

H.5.6.3 Geometry and Style of Faulting

There are two alternative geometries for the ERM-S RLME source: ERM-SCC (weight of 0.6) and the ERM-SRP (weight 0.4). These are shown on Figure H-5.6-3. A single geometry is specified for the ERM-N RLME source.

The probability distribution used to model seismogenic thickness for the ERM-S and ERM-N RLME sources is: 13 km (weight of 0.3), 15 km (weight of 0.5), and 17 km (weight of 0.2).

Future ruptures are to be modeled as vertical strike slip ruptures aligned parallel with the long axis to the RLME source zones. Both the northeastern and southwestern ends of the zones are modeled as leaky to allow for uncertainty in the extent of possible reactivated faults along the rift margin.

H.5.6.4 RLME Magnitude

Tables H-5.6-1 and H-5.6-2 list the RLME magnitude distributions for the ERM-S and ERM-N RLMEs, respectively. Aleatory variability in the size of an RLME is modeled as a uniform distribution of ±0.25 **M** units centered on the expected RLME magnitude value given in the tables.

H.5.6.5 RLME Recurrence

The remaining nodes of the ERM-S and ERM-N logic trees address the estimation of recurrence rate of RLMEs.

Recurrence Method

The "Earthquake Count in a Time Interval" approach is used to assess RLME recurrence frequency for both the ERM-S and ERM-N sources.

Recurrence Data

For the ERM-S source, three alternative data sets are used to assess RLME recurrence rates: either two, three, or four earthquakes in a 17.7 to 21.7 ka period. The three alternatives have equal weight.

For the ERM-N source, two alternative data sets are use: either one (weight 0.9) or two (weight 0.1) earthquakes in a 12–35 ka period.

Earthquake Recurrence Model

The Poisson model is used as the default earthquake recurrence model with weight 1.0 for both the ERM-S and ERM-N sources.

RLME Annual Frequency

Tables H-5.6-3, H-5.6-4, and H-5.6-5 list the distribution of RLME recurrence frequencies for the ERM-S source. Tables H-5.6-6 and H-5.6-7 list the distribution of RLME recurrence frequencies for the ERM-N source.

H.5.7 Marianna Zone RLME Seismic Source Model

The Marianna Zone RLME is described in Section 6.1.7 of the main report. The logic tree for this source is shown on Figure H-5.7-1. The data for this source is contained on the CEUS SSC Project web site in file "Marianna_RLME.xls."

H.5.7.1 Temporal Clustering

The first node of the logic tree for the RLME source (Figure H-5.7-1) addresses the issue of temporal clustering of earthquakes. The in-cluster model is assigned a weight of 0.5 and the out-of-cluster model is assigned a weight of 0.5. For the "in" branch, the remaining portion of the logic tree is used to define the hazard from this source. On the "out" branch the Marianna RLME source is not included in calculation of the total seismic hazard.

H.5.7.2 Localizing Feature

RLMEs are modeled as occurring randomly with the boundary of the Marianna zone shown on Figure H-5.7-2.

H.5.7.3 Geometry and Style of Faulting

A single geometry for the Marianna RLME source is used. The geometry is shown on Figure H-5.7-2.

The probability distribution used to model seismogenic thickness is 13 km (weight of 0.3), 15 km (weight of 0.5), or 17 km (weight of 0.2).

Two equally weighted alternatives for future ruptures of RLMEs are modeled: either vertical strike-slip ruptures oriented northeast parallel to the sides of the Marianna zone or vertical strike-slip ruptures oriented northwest parallel to the sides of the Marianna zone. All boundaries to the MAR zone are leaky.

H.5.7.4 RLME Magnitude

The distribution for RLME magnitude for the Marianna RLME source is given in Table H-5.7-1. Aleatory variability in the size of an RLME is modeled as a uniform distribution of ±0.25 **M** units centered on the expected RLME magnitude value given in the table.

H.5.7.5 RLME Recurrence

The remaining branches of the logic tree describe the assessment of RLME recurrence rates.

Recurrence Method

The "Earthquake Recurrence Intervals" approach is used with weight 1.0 (Figure H-5.7-1).

Recurrence Data

The two equally weighted data sets consist of either three or four earthquakes with the oldest occurring approximately 9.9 ka.

Earthquake Recurrence Model

The Poisson model is used as the default earthquake recurrence model with weight 1.0 for the Marianna RLME source.

RLME Annual Frequency

The final node of the logic tree addresses the uncertainty distributions for the annual frequency of RLMEs. These distributions are given in Tables H-5.7-2 and H-5.7-3.

H.5.8 Commerce Fault RLME Seismic Source Model

The Commerce RLME source is described in Section 6.1.8 of the main text. The source logic tree is shown on Figure H-5.8-1. The data for this source is contained on the CEUS SSC Project web site in file "Commerce_RLME.xls."

H.5.8.1 Temporal Clustering

This node of the logic tree is not applicable to this source.

H.5.8.2 Localizing Feature

RLMEs are modeled as occurring randomly with the boundary of the Commerce zone shown on Figure H-5.8-2.

H.5.8.2 Geometry and Style of Faulting

A single geometry for the Commerce RLME source is modeled.

The uncertainty distribution for seismogenic crustal thickness is: 13 km (weight of 0.3), 15 km (weight of 0.5), or 17 km (weight of 0.2).

The Commerce RLME source is modeled as a zone of vertical strike-slip faulting. Ruptures are to be oriented N47°E, subparallel to the Commerce zone boundary. The northeast and southwest boundaries of the zone are considered leaky boundaries.

H.5.8.4 RLME Magnitude

Table H-5.8-1 lists the uncertainty distribution for the Commerce RLME magnitude. Aleatory variability in the size of an RLME is modeled as a uniform distribution of ±0.25 **M** units centered on the expected RLME magnitude value given in the table.

H.5.8.5 RLME Recurrence

The remaining branches of the logic tree describe the assessment of RLME recurrence rates.

Recurrence Method

The “Earthquake Recurrence Intervals” approach is used with weight 1.0 (Figure H-5.8-1).

Recurrence Data

The preferred interpretation (weight 0.75) is that two earthquakes have occurred in the past 23 kyr with the possibility (weight 0.25) that the count is three earthquakes.

Earthquake Recurrence Model

The Poisson model is used as the earthquake recurrence model with weight 1.0 for the Commerce RLME source.

RLME Annual Frequency

Tables H-5.8-2 and H-5.8-3 list the alternative distributions for RLME frequency for the Commerce RLME source.

H.5.9 Wabash Valley RLME Seismic Source Model

The Wabash Valley RLME source is described in Section 6.1.9 of the main text. The source logic tree is shown on Figure H-5.9-1. The data for this source is contained on the CEUS SSC Project web site in file "Wabash_RLME.xls."

H.5.9.1 Temporal Clustering

This node of the logic tree is not applicable to this source.

H.5.9.2 Localizing Feature

RLMEs are modeled as occurring randomly with the boundary of the Wabash Valley zone shown on Figure H-5.9-2.

H.5.9.3 Geometry and Style of Faulting

A single zone geometry is used to model the Wabash Valley RLME. This geometry is shown on Figure H-5.9-2.

Two alternative estimates of the seismogenic thickness of the crust in the Wabash Valley RLME are used: 17 km (weight of 0.7) or 22 km (weight of 0.3).

The boundaries of the Wabash Valley RLME source zone are modeled as leaky. Earthquakes are to be modeled with a random strike (uniform 0º to 360º azimuth). The earthquakes are a mixture of 2/3 vertical strike-slip and 1/3 reverse (random dip in the range of 40º to 60º)

H.5.9.4 RLME Magnitude

Table H-5.9-1 lists the uncertainty distribution for the magnitude of Wabash Valley RLMEs. Aleatory variability in the size of an RLME is modeled as a uniform distribution of ±0.25 **M** units centered on the expected RLME magnitude value given in the table.

H.5.9.5 RLME Recurrence

The remaining branches of the logic tree describe the assessment of RLME recurrence rates.

Recurrence Method

The "Earthquake Recurrence Intervals" approach is used with weight 1.0 (Figure H-5.9-1).

Recurrence Data

The available data for characterizing the recurrence rate of Wabash Valley RLMEs are the estimated ages for the Vincennes-Bridgeport and Skelton paleoearthquakes.

Earthquake Recurrence Model

The Poisson model is used as the earthquake recurrence model with weight 1.0 for the Wabash Valley RLME source.

RLME Annual Frequency

The final node of the logic tree addresses the uncertainty distributions for the annual frequency of RLMEs. This distribution is listed in Table H-5.9-2.

Table H-3-1
Weighted Alternative Seismogenic Crustal Thickness Values for Mmax Zones

Mmax Zone	Crustal Thickness and [Weight]
Study Region	13 km [0.4], 17 km [0.4], 22 km [0.2]
MESE-W	13 km [0.4], 17 km [0.4], 22 km [0.2]
MESE-N	13 km [0.4], 17 km [0.4], 22 km [0.2]
NMESE-W	13 km [0.4], 17 km [0.4], 22 km [0.2]
NMESE-N	13 km [0.4], 17 km [0.4], 22 km [0.2]

Table H-3-2
Aleatory Distributions for Characterization of Future Earthquake Ruptures for Mmax Zones

Mmax Zone	Source Boundary Characteristics	Sense of Slip (Relative Frequency)	Rupture Strike (Relative Frequency)	Rupture Dip (Relative Frequency)
Study Region, MESE-N, MESE-W, NMESE-N, NMESE-W	Leaky[a]	Strike-slip (2/3)	N50W (0.2) N00E (0.2) N35E (0.4) N60E (0.1) N90E (0.1)	Uniformly distributed 60º to 90º, equally likely dip direction
		Reverse (1/3)	N50W (0.2) N00E (0.2) N35E (0.4) N60E (0.1) N90E (0.1)	Uniformly distributed 30º to 60º, equally likely dip direction

[a] Leaky boundary denotes the case were earthquake ruptures are centered on the earthquake epicenter, the epicenters are contained within the source boundary, but the rupture is allowed to extend beyond the source boundary.

Table H-3-3
Maximum Magnitude Distributions for Mmax Distributed Seismicity Sources

Weight Assigned to Mmax	Maximum Magnitude for:				
	Study Region	MESE_N	NMESE_N	MESE_W	NMESE_W
0.101	6.5	6.4	6.4	6.5	5.7
0.244	6.9	6.8	6.8	6.9	6.1
0.310	7.2	7.2	7.1	7.3	6.6
0.244	7.7	7.7	7.5	7.7	7.2
0.101	8.1	8.1	8.0	8.1	7.9

Table H-4-1
Seismotectonic Source Zones

Zone Acronym	Seismotectonic Source Zone
AHEX	Atlantic Highly Extended Crust
ECC-AM	Extended Continental Crust—Atlantic Margin
ECC-GC	Extended Continental Crust—Gulf Coast
GMH	Great Meteor Hotspot
IBEB	Illinois Basin Extended Basement
GHEX	Gulf Highly Extended Crust
MidC-A, MidC-B, MidC-C, MidC-D	Midcontinent-Craton alternatives
OKA	Oklahoma Aulacogen
PEZ-N and PEZ-W	Paleozoic Extended Crust narrow and Paleozoic Extended Crust wide
RR and RR-RCG	Reelfoot Rift and Reelfoot Rift including the Rough Creek Graben
SLR	St. Lawrence Rift, including the Ottawa and Saguenay grabens

Table H-4-2
Weighted Alternative Seismogenic Crustal Thickness Values for Seismotectonic Zones

Mmax Zone	Crustal Thickness and [Weight]
AHEX, GHEX	8 km [0.5], 15 km [0.5]
ECC-AM, ECC-GC, MidC-A, MidC-B, MidC-C, MidC-D, IBEB, NAP,PEZ-N, PEZ-W	13 km [0.4], 17 km [0.4], 22 km [0.2]
GMH, SLR	25 km [0.5], 30 km [0.5]
OKA	15 km [0.5] 20 km [0.5]
RR, RR-RCG	13 km [0.4], 15 km [0.4], 17 km [0.2]

Table H-4-3
Aleatory Distributions for Characterization of Future Earthquake Ruptures for Seismotectonic Zones

Seismotectonic Zone	Source Boundary Characteristics	Sense of Slip (Relative Frequency)	Rupture Strike (Relative Frequency)	Rupture Dip (Relative Frequency)
AHEX, ECC-AM, MidC-A, MidC-B, MidC-C, MidC-D, PEZ-N, PEZ-W	Leaky[a]	Strike-slip (2/3)	N50W (0.2) N00E (0.2) N35E (0.4) N60E (0.1) N90E (0.1)	Uniformly distributed 60º to 90º, equally likely dip direction
		Reverse (1/3)	N50W (0.2) N00E (0.2) N35E (0.4) N60E (0.1) N90E (0.1)	Uniformly distributed 30º to 60º, equally likely dip direction
ECC-GC, GHEX	Leaky[a]	Strike-slip (2/3)	Uniform 0º to 180º	Uniformly distributed 60º to 90º, equally likely dip direction
		Reverse (1/3)	Uniform 0º to 180º	Uniformly distributed 30º to 60º, equally likely dip direction
GMH	Leaky[a]	Strike-slip (0.2)	N40W (0.4) N20E (0.4) N90E (0.1)	Uniformly distributed 60º to 90º, equally likely dip direction
		Reverse (0.8)	N40W (0.4) N20E (0.4) N90E (0.1)	Uniformly distributed 30º to 60º, equally likely dip direction
IBEB	Leaky[a]	Reverse Oblique (0.1)	N20W (1.0)	75ºE (0.5) 75ºW (0.5)
		Reverse (0.3)	N00E (1.0)	40ºE (0.2) 40ºW (0.2) 75ºE (0.3) 75ºW (0.3)
		Strike-slip (0.6)	N50W (0.167) N90E (0.333) N40E (0.5)	90º (1.0)
NAP	Leaky[a]	Strike-slip (1/3)	N50W (0.2) N00E (0.2) N35E (0.4) N60E (0.1) N90E (0.1)	Uniformly distributed 60º to 90º, equally likely dip direction

Seismotectonic Zone	Source Boundary Characteristics	Sense of Slip (Relative Frequency)	Rupture Strike (Relative Frequency)	Rupture Dip (Relative Frequency)
		Reverse (2/3)	N50W (0.2) N00E (0.2) N35E (0.4) N60E (0.1) N90E (0.1)	Uniformly distributed 30º to 60º, equally likely dip direction
OKA	Leaky[a]	Reverse Oblique (1.0)	Parallel to Long Axis of Zone (1.0)	Uniform 45ºN to 75ºN (0.5) Uniform 45ºS to 75ºS (0.5)
RR, RR-RCG	Leaky[a]	Reverse (0.35)	N10W (1.0)	40ºE (0.25) 40ºW (0.25) 70ºE (0.25) 70ºE (0.25)
		Strike-slip (0.65)	N50W (0.3) N30E (0.3) N55E (0.3) N90E (0.1)	90º (1.0)
SLR	Leaky[a]	Strike-slip (1/3)	N25E (0.2) N40E (0.2) N70E (0.2) N50W (0.15) N70W (0.15) NS (0.05) EW (0.05)	Uniformly distributed 60º to 90º, equally likely dip direction
		Reverse (2/3)	N25E (0.2) N40E (0.2) N70E (0.2) N50W (0.15) N70W (0.15) NS (0.05) EW (0.05)	Uniformly distributed 30º to 60º, equally likely dip direction

[a] Leaky boundary denotes the case were earthquake ruptures are centered on the earthquake epicenter, the epicenters are contained within the source boundary, but the rupture is allowed to extend beyond the source boundary.

Table H-4-4
Maximum Magnitude Distributions for Seismotectonic Distributed Seismicity Sources

Weight	Maximum Magnitude for:												
	AHEX	ECC-AM	ECC-GC	GHEX	GMH	IBEB	MidC-A, MidC-B, MidC-C, and MidC-D	NAP	OKA	PEZ-N and PEZ-W	RR	RR-RCG	SLR
0.101	6.0	6.0	6.0	6.0	6.0	6.5	5.6	6.1	5.8	5.9	6.2	6.1	6.2
0.244	6.7	6.7	6.7	6.7	6.7	6.9	6.1	6.7	6.4	6.4	6.7	6.6	6.8
0.310	7.2	7.2	7.2	7.2	7.2	7.4	6.6	7.2	6.9	6.8	7.2	7.1	7.3
0.244	7.7	7.7	7.7	7.7	7.7	7.8	7.2	7.7	7.4	7.2	7.7	7.6	7.7
0.101	8.1	8.1	8.1	8.1	8.1	8.1	8.0	8.1	8.0	7.9	8.1	8.1	8.1

Table H-5.1-1
Charlevoix RLME Magnitude Distribution

Moment Magnitude	Weight
6.75	0.2
7.0	0.5
7.25	0.2
7.5	0.1

Table H-5.1-2
Annual Frequencies for Charlevoix RLME Events
Data Set 1: 1870 and 1663

RLME Frequency (Events/Year)	Weight
9.3E-03	0.101
6.7E-03	0.244
4.2E-03	0.310
2.2E-03	0.244
7.7E-04	0.101

Table H-5.1-3
Annual Frequencies for Charlevoix RLME Events
Data Set 2: 3 Earthquakes in 6–7 kyr BP

RLME Frequency (Events/Year)	Weight
1.3E-03	0.101
8.4E-04	0.244
5.7E-04	0.310
3.7E-04	0.244
1.9E-04	0.101

Table H-5.1-4
Annual Frequencies for Charlevoix RLME Events
Data Set 3: 4 Earthquakes in 9.5–10.2 kyr BP

RLME Frequency (Events/Year)	Weight
9.8E-04	0.101
6.7E-04	0.244
4.7E-04	0.310
3.2E-04	0.244
1.8E-04	0.101

Table H-5.2-1
Charleston RLME Magnitude Distribution

Moment Magnitude	Weight
6.7	0.10
6.9	0.25
7.1	0.30
7.3	0.25
7.5	0.10

Table H-5.2-2
Annual Frequencies for Charleston RLME Events
Poisson Model, 2,000-Year Time Period
Earthquakes 1886, A, B, and C

RLME Frequency (Events/Year)	Weight
4.7E-03	0.101
3.1E-03	0.244
2.1E-03	0.310
1.3E-03	0.244
6.8E-04	0.101

Table H-5.2-3
Annual Frequencies for Charleston RLME Events
Poisson Model, 5,500-Year Time Period
Earthquakes 1886, A, B, and C

RLME Frequency (Events/Year)	Weight
4.7E-03	0.101
3.1E-03	0.244
2.1E-03	0.310
1.3E-03	0.244
6.8E-04	0.101

Table H-5.2-4
Annual Frequencies for Charleston RLME Events
Poisson Model, 5,500-Year Time Period
Earthquakes 1886, A, B, C, and D

RLME Frequency (Events/Year)	Weight
2.7E-03	0.101
1.9E-03	0.244
1.3E-03	0.310
8.8E-04	0.244
5.0E-04	0.101

Table H-5.2-5
Annual Frequencies for Charleston RLME Events
Poisson Model, 5,500-Year Time Period
Earthquakes 1886, A, B, C, and E

RLME Frequency (Events/Year)	Weight
1.9E-03	0.101
1.3E-03	0.244
9.2E-04	0.310
6.4E-04	0.244
3.4E-04	0.101

Table H-5.2-6
Annual Frequencies for Charleston RLME Events
Poisson Model, 5,500-Year Time Period
Earthquakes 1886, A, B, C, D, and E

RLME Frequency (Events/Year)	Weight
2.2E-03	0.101
1.5E-03	0.244
1.1E-03	0.310
7.8E-04	0.244
4.6E-04	0.101

Table H-5.2-7
Annual Frequencies for Charleston RLME Events
BPT Renewal Model, α = 0.3, 2,000-Year Time Period
Earthquakes 1886, A, B, and C

RLME Frequency (Events/Year)	Weight
6.4E-05	0.101
7.6E-06	0.244
9.5E-07	0.310
8.5E-08	0.244
2.3E-09	0.101

Table H-5.2-8
Annual Frequencies for Charleston RLME Events
BPT Renewal Model, α = 0.5, 2,000-Year Time Period
Earthquakes 1886, A, B, and C

RLME Frequency (Events/Year)	Weight
1.4E-03	0.101
3.8E-04	0.244
9.5E-05	0.310
1.7E-05	0.244
1.0E-06	0.101

Table H-5.2-9
Annual Frequencies for Charleston RLME Events
BPT Renewal Model, α = 0.7, 2,000-Year Time Period
Earthquakes 1886, A, B, and C

RLME Frequency (Events/Year)	Weight
2.6E-03	0.101
9.8E-04	0.244
3.2E-04	0.310
7.1E-05	0.244
5.6E-06	0.101

Table H-5.2-10
Annual Frequencies for Charleston RLME Events
BPT Renewal Model, α = 0.3, 5,500-Year Time Period
Earthquakes 1886, A, B, and C

RLME Frequency (Events/Year)	Weight
6.8E-05	0.101
8.0E-06	0.244
1.0E-06	0.310
9.2E-08	0.244
2.5E-09	0.101

Table H-5.2-11
Annual Frequencies for Charleston RLME Events
BPT Renewal Model, α = 0.5, 5,500-Year Time Period
Earthquakes 1886, A, B, and C

RLME Frequency (Events/Year)	Weight
1.4E-03	0.101
3.9E-04	0.244
9.8E-05	0.310
1.7E-05	0.244
1.1E-06	0.101

Table H-5.2-12
Annual Frequencies for Charleston RLME Events
BPT Renewal Model, α = 0.7, 5,500-Year Time Period
Earthquakes 1886, A, B, and C

RLME Frequency (Events/Year)	Weight
2.7E-03	0.101
9.9E-04	0.244
3.3E-04	0.310
7.3E-05	0.244
5.8E-06	0.101

Table H-5.2-13
Annual Frequencies for Charleston RLME Events
BPT Renewal Model, α = 0.3, 5,500-Year Time Period
Earthquakes 1886, A, B, C, and D

RLME Frequency (Events/Year)	Weight
3.5E-07	0.101
2.5E-08	0.244
2.2E-09	0.310
1.4E-10	0.244
2.7E-12	0.101

Table H-5.2-14
Annual Frequencies for Charleston RLME Events
BPT Renewal Model, α = 0.5, 5,500-Year Time Period
Earthquakes 1886, A, B, C, and D

RLME Frequency (Events/Year)	Weight
2.2E-04	0.101
4.5E-05	0.244
9.3E-06	0.310
1.4E-06	0.244
7.6E-08	0.101

Table H-5.2-15
Annual Frequencies for Charleston RLME Events
BPT Renewal Model, $\alpha = 0.7$, 5,500-Year Time Period
Earthquakes 1886, A, B, C, and D

RLME Frequency (Events/Year)	Weight
1.0E-03	0.101
3.3E-04	0.244
9.5E-05	0.310
2.0E-05	0.244
1.5E-06	0.101

Table H-5.2-16
Annual Frequencies for Charleston RLME Events
BPT Renewal Model, $\alpha = 0.3$, 5,500-Year Time Period
Earthquakes 1886, A, B, C, and E

RLME Frequency (Events/Year)	Weight
4.5E-09	0.101
2.0E-10	0.244
1.2E-11	0.310
5.4E-13	0.244
6.4E-15	0.101

Table H-5.2-17
Annual Frequencies for Charleston RLME Events
BPT Renewal Model, $\alpha = 0.5$, 5,500-Year Time Period
Earthquakes 1886, A, B, C, and E

RLME Frequency (Events/Year)	Weight
5.2E-05	0.101
8.2E-06	0.244
1.4E-06	0.310
1.7E-07	0.244
7.0E-09	0.101

Table H-5.2-18
Annual Frequencies for Charleston RLME Events
BPT Renewal Model, α = 0.7, 5,500-Year Time Period
Earthquakes 1886, A, B, C, and E

RLME Frequency (Events/Year)	Weight
5.2E-04	0.101
1.4E-04	0.244
3.4E-05	0.310
6.1E-06	0.244
3.9E-07	0.101

Table H-5.2-19
Annual Frequencies for Charleston RLME Events
BPT Renewal Model, α = 0.3, 5,500-Year Time Period
Earthquakes 1886, A, B, C, D, and E

RLME Frequency (Events/Year)	Weight
1.5E-08	0.101
8.7E-10	0.244
7.0E-11	0.310
4.4E-12	0.244
8.2E-14	0.101

Table H-5.2-20
Annual Frequencies for Charleston RLME Events
BPT Renewal Model, α = 0.5, 5,500-Year Time Period
Earthquakes 1886, A, B, C, D, and E

RLME Frequency (Events/Year)	Weight
7.0E-05	0.101
1.3E-05	0.244
2.5E-06	0.310
3.7E-07	0.244
2.1E-08	0.101

Table H-5.2-21
Annual Frequencies for Charleston RLME Events
BPT Renewal Model, α = 0.7, 5,500-Year Time Period
Earthquakes 1886, A, B, C, D, and E

RLME Frequency (Events/Year)	Weight
5.7E-04	0.101
1.6E-04	0.244
4.5E-05	0.310
9.2E-06	0.244
7.6E-07	0.101

Table H-5.3-1
Cheraw RLME Magnitude Distribution

Moment Magnitude	Weight
6.8	0.3
7.0	0.3
7.2	0.3
7.4	0.1

Table H-5.3-2
Annual Frequencies for Cheraw RLME Events
In-Cluster Case, Data Set: 2 Earthquakes in 20–25 kyr

RLME Frequency (Events/Year)	Weight
2.4E-04	0.101
1.3E-04	0.244
7.6E-05	0.310
3.8E-05	0.244
1.4E-05	0.101

Table H-5.3-3
Annual Frequencies for Cheraw RLME Events
In-Cluster Case, Data Set: 3 Earthquakes in 20–25 kyr

RLME Frequency (Events/Year)	Weight
3.1E-04	0.101
1.9E-04	0.244
1.2E-04	0.310
7.2E-05	0.244
3.2E-05	0.101

Table H-5.3-4
Slip Rates for Cheraw Fault
In-Cluster Case, Data Set: 3.2–4.1 m in 20–25 kyr

RLME Fault Slip Rate (mm/Year)	Weight
0.14	0.185
0.16	0.630
0.19	0.185

Table H-5.3-5
Annual Frequencies for Cheraw RLME Events
Out-of-Cluster Case, Time Between Clusters

RLME Frequency (Events/Year)	Weight
5.0E-06	0.333
2.9E-06	0.334
2.0E-06	0.333

Table H-5.3-6
Slip Rates for Cheraw Fault
Out-of-Cluster Case, Data Set: 7–8 m in 0.4–2.0 myr

RLME Fault Slip Rate (mm/Year)	Weight
0.0038	0.101
0.0043	0.244
0.0054	0.310
0.0072	0.244
0.011	0.101

Table H-5.4-1
Meers RLME Magnitude Distribution

Moment Magnitude	Weight
6.6	0.1
6.7	0.45
6.9	0.3
7.3	0.1
7.4	0.05

Table H-5.4-2
Annual Frequencies for Meers RLME Events
In-Cluster Case

RLME Frequency (Events/Year)	Weight
2.1E-03	0.101
1.2E-03	0.244
6.7E-04	0.310
3.4E-04	0.244
1.2E-04	0.101

Table H-5.4-3
Annual Frequencies for Meers RLME Events
Out-of-Cluster Case

RLME Frequency (Events/Year)	Weight
5.0E-06	0.333
2.9E-06	0.334
2.0E-06	0.333

Table H-5.5-1
NMFS RLME Magnitude Distribution

Moment Magnitude for:			Weight
NMS	RFT	NMN	
7.9	7.8	7.6	0.167
7.8	7.7	7.5	0.167
7.6	7.8	7.5	0.250
7.2	7.4	7.2	0.083
6.9	7.3	7.0	0.250
6.7	7.1	6.8	0.083

Table H-5.5-2
Annual Frequencies for NMFS RLME Events
In-Cluster Case, Poisson Model

RLME Frequency (Events/Year)	Weight
6.0E-03	0.101
3.7E-03	0.244
2.4E-03	0.310
1.4E-03	0.244
6.2E-04	0.101

Table H-5.5-3
Annual Frequencies for NMFS RLME Events
In-Cluster Case, BPT Model, α = 0.3

RLME Frequency (Events/Year)	Weight
3.5E-03	0.101
1.1E-03	0.244
3.2E-04	0.310
6.4E-05	0.244
4.7E-06	0.101

Table H-5.5-4
Annual Frequencies for NMFS RLME Events
In-Cluster Case, BPT Model, α = 0.5

RLME Frequency (Events/Year)	Weight
4.8E-03	0.101
2.2E-03	0.244
8.9E-04	0.310
2.6E-04	0.244
3.1E-05	0.101

Table H-5.5-5
Annual Frequencies for NMFS RLME Events
In-Cluster Case, BPT Model, α = 0.7

RLME Frequency (Events/Year)	Weight
4.4E-03	0.101
2.2E-03	0.244
1.0E-03	0.310
3.4E-04	0.244
4.7E-05	0.101

Table H-5.5-6
Annual Frequencies for NMFS RLME Events
Out-of-Cluster Case, Poisson Model

RLME Frequency (Events/Year)	Weight
1.3E-03	0.101
7.2E-04	0.244
4.2E-04	0.310
2.2E-04	0.244
8.0E-05	0.101

Table H-5.6-1
ERM-S RLME Magnitude Distribution

Moment Magnitude	Weight
6.7	0.15
6.9	0.2
7.1	0.2
7.3	0.2
7.5	0.2
7.7	0.05

Table H-5.6-2
ERM-N RLME Magnitude Distribution

Moment Magnitude	Weight
6.7	0.3
6.9	0.3
7.1	0.3
7.4	0.1

Table H-5.6-3
Annual Frequencies for ERM-S RLME Events
Data Set: 2 Earthquakes in 17.7–21.7 kyr

RLME Frequency (Events/Year)	Weight
3.5E-04	0.101
2.1E-04	0.244
1.4E-04	0.310
8.0E-05	0.244
3.6E-05	0.101

Table H-5.6-4
Annual Frequencies for ERM-S RLME Events
Data Set: 3 Earthquakes in 17.7–21.7 kyr

RLME Frequency (Events/Year)	Weight
4.3E-04	0.101
2.8E-04	0.244
1.9E-04	0.310
1.2E-04	0.244
6.2E-05	0.101

Table H-5.6-5
Annual Frequencies for ERM-S RLME Events
Data Set: 4 Earthquakes in 17.7–21.7 kyr

RLME Frequency (Events/Year)	Weight
5.0E-04	0.101
3.4E-04	0.244
2.4E-04	0.310
1.6E-04	0.244
9.0E-05	0.101

Table H-5.6-6
Annual Frequencies for ERM-N RLME Events
Data Set: 1 Earthquake in 12–35 kyr

RLME Frequency (Events/Year)	Weight
2.9E-04	0.101
1.5E-04	0.244
8.0E-05	0.310
4.0E-05	0.244
1.4E-05	0.101

Table H-5.6-7
Annual Frequencies for ERM-N RLME Events
Data Set: 2 Earthquakes in 12–35 kyr

RLME Frequency (Events/Year)	Weight
3.9E-04	0.101
2.2E-04	0.244
1.3E-04	0.310
7.2E-05	0.244
3.2E-05	0.101

Table H-5.7-1
Marianna RLME Magnitude Distribution

Moment Magnitude	Weight
6.7	0.15
6.9	0.2
7.1	0.2
7.3	0.2
7.5	0.2
7.7	0.05

Table H-5.7-2
Annual Frequencies for Marianna RLME Events
Data Set: 3 Earthquakes in 9.6–10.2 kyr

RLME Frequency (Events/Year)	Weight
6.9E-04	0.101
4.2E-04	0.244
2.7E-04	0.310
1.6E-04	0.244
7.2E-05	0.101

Table H-5.7-3
Annual Frequencies for Marianna RLME Events
Data Set: 4 Earthquakes in 9.6–10.2 kyr

RLME Frequency (Events/Year)	Weight
8.4E-04	0.101
5.5E-04	0.244
3.7E-04	0.310
2.4E-04	0.244
1.2E-04	0.101

Table H-5.8-1
Commerce RLME Magnitude Distribution

Moment Magnitude	Weight
6.7	0.15
6.9	0.35
7.1	0.35
7.3	0.10
7.7	0.05

Table H-5.8-2
Annual Frequencies for Commerce RLME Events
Data Set: 2 Earthquakes in 18.9–23.6 kyr

RLME Frequency (Events/Year)	Weight
2.5E-04	0.101
1.4E-04	0.244
8.0E-05	0.310
4.0E-05	0.244
1.4E-05	0.101

Table H-5.8-3
Annual Frequencies for Commerce RLME Events
Data Set: 3 Earthquakes in 18.9–23.6 kyr

RLME Frequency (events/Year)	Weight
3.3E-04	0.101
2.0E-04	0.244
1.3E-04	0.310
7.6E-05	0.244
3.4E-05	0.101

Table H-5.9-1
Wabash RLME Magnitude Distribution

Moment Magnitude	Weight
6.75	0.05
7.0	0.25
7.25	0.35
7.5	0.35

Table H-5.9-2
Annual Frequencies for Wabash RLME Events
Data Set: 2 Earthquakes in 11–13 kyr

RLME Frequency (Events/Year)	Weight
4.4E-04	0.101
2.5E-04	0.244
1.4E-04	0.310
7.2E-05	0.244
2.4E-05	0.101

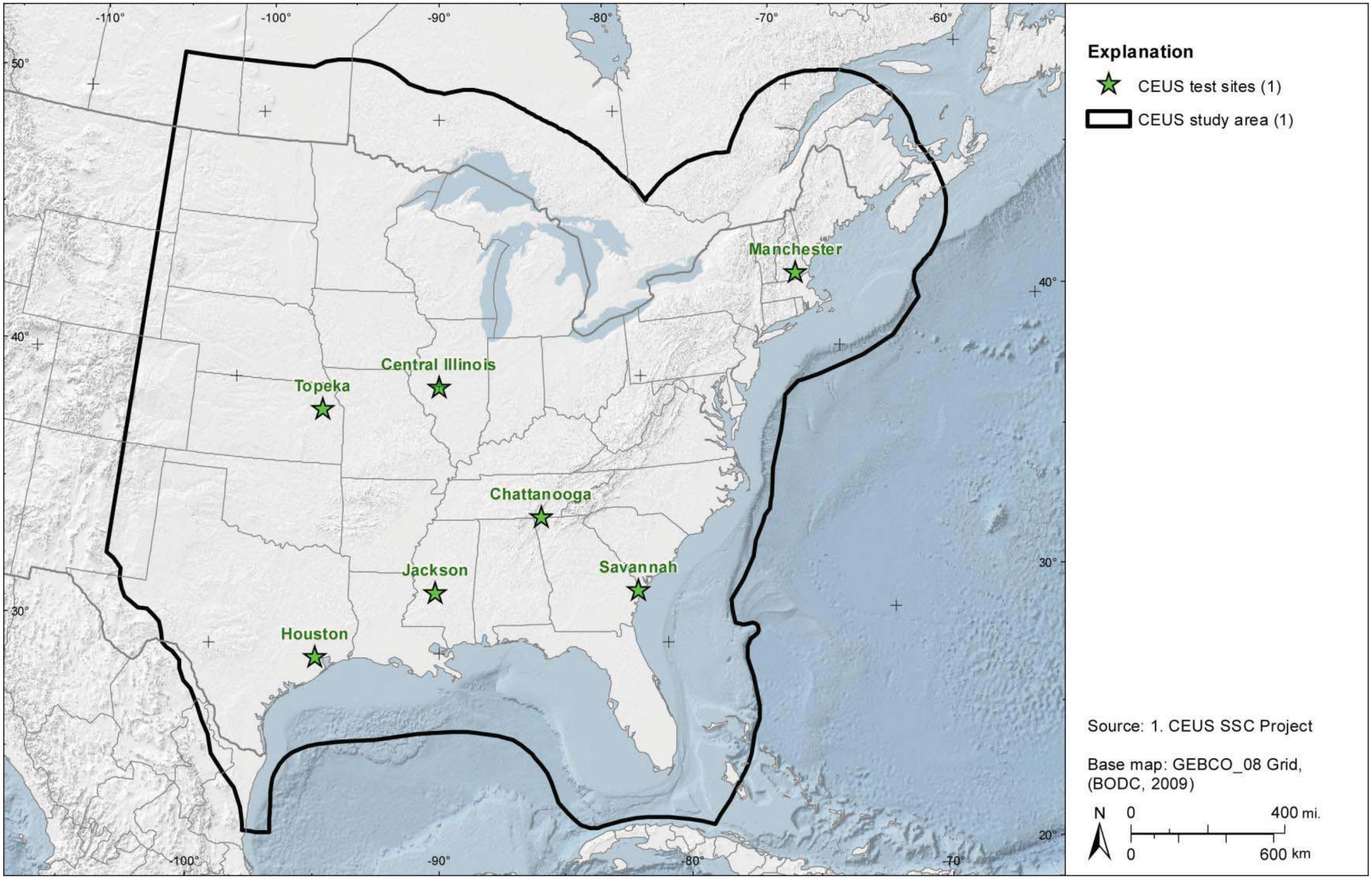

Figure H-1-1
Region covered by the CEUS SSC model

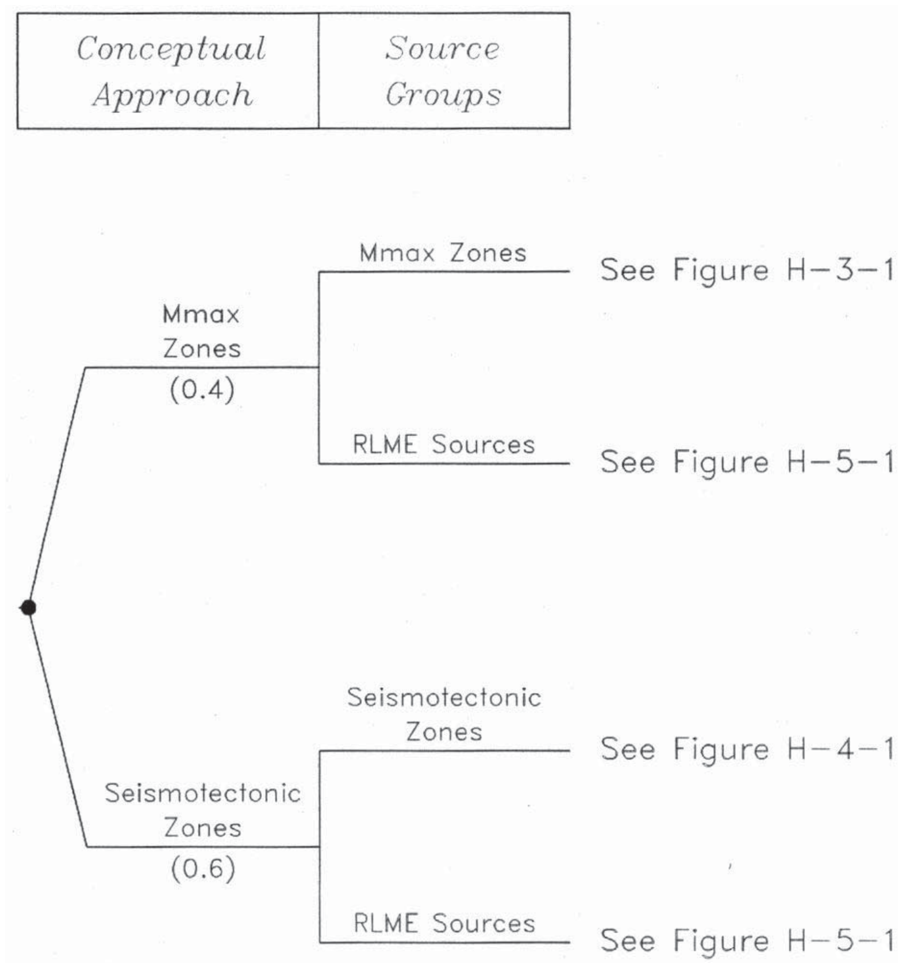

Figure H-2-1
Master logic tree for the CEUS SSC model

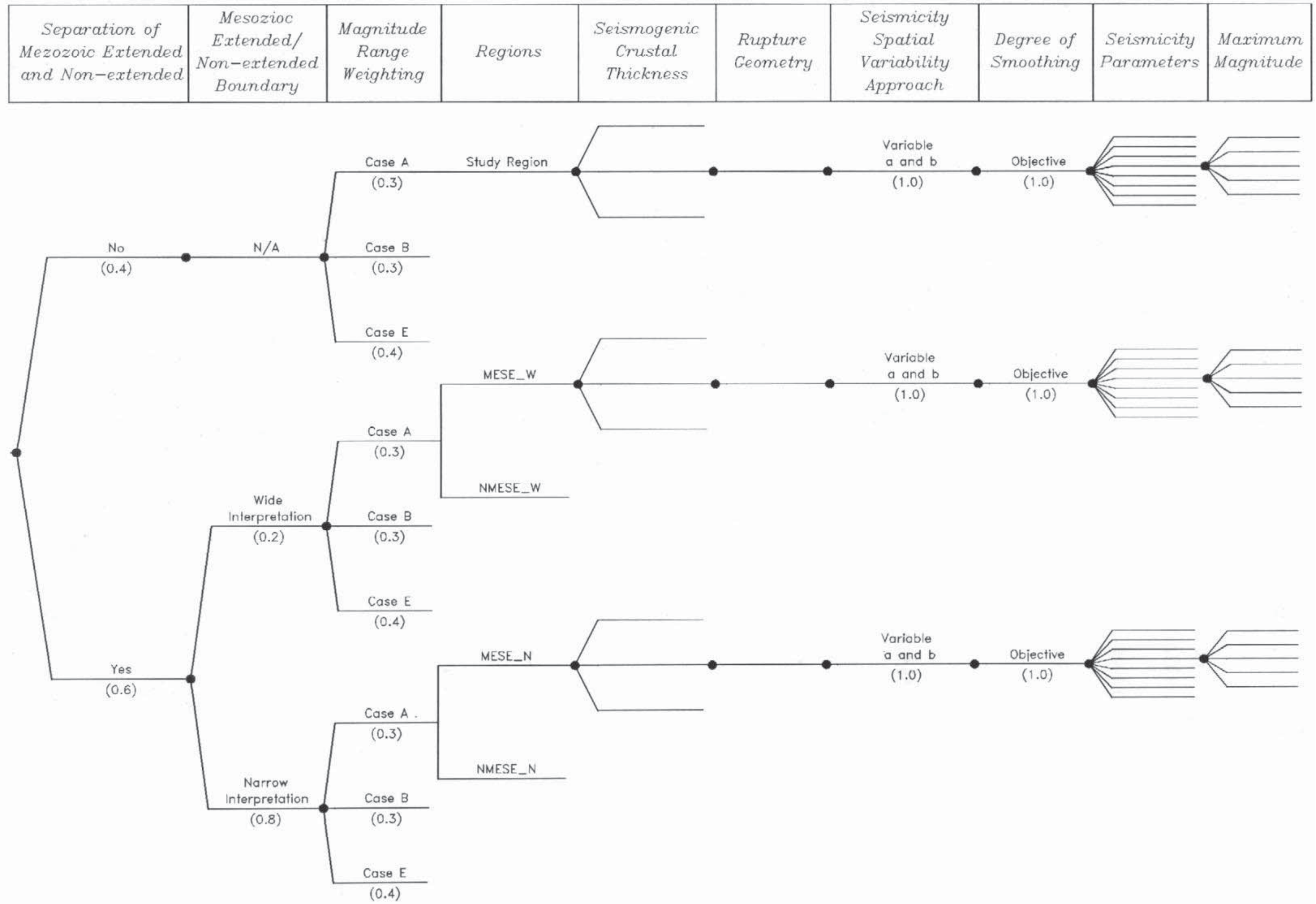

Figure H-3-1
Logic tree for the Mmax zones branch of the master logic tree

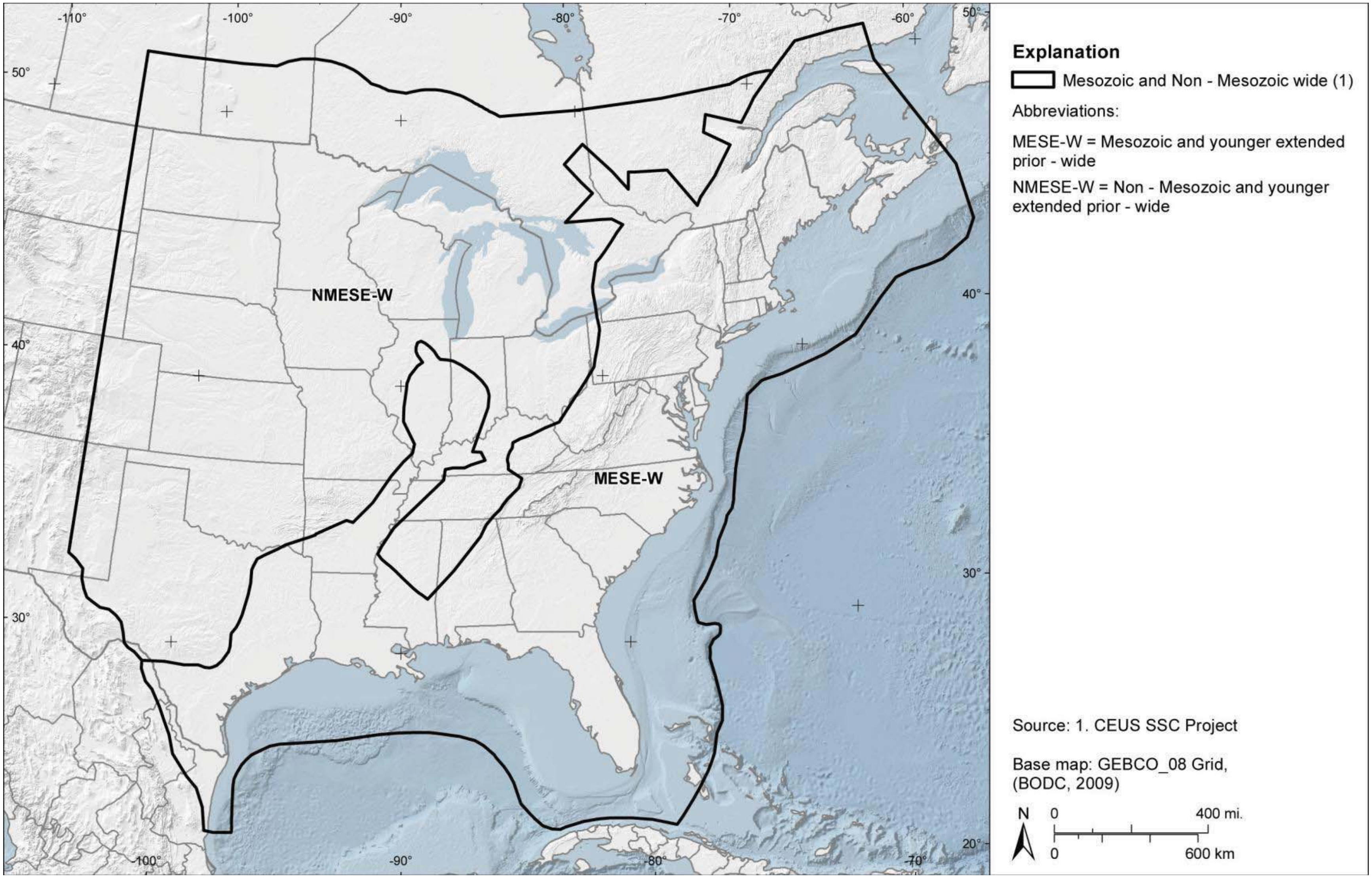

Figure H-3-2
Mesozoic extended (MESE-W) and non-extended (NMESE-W) Mmax zones for the "wide" interpretation

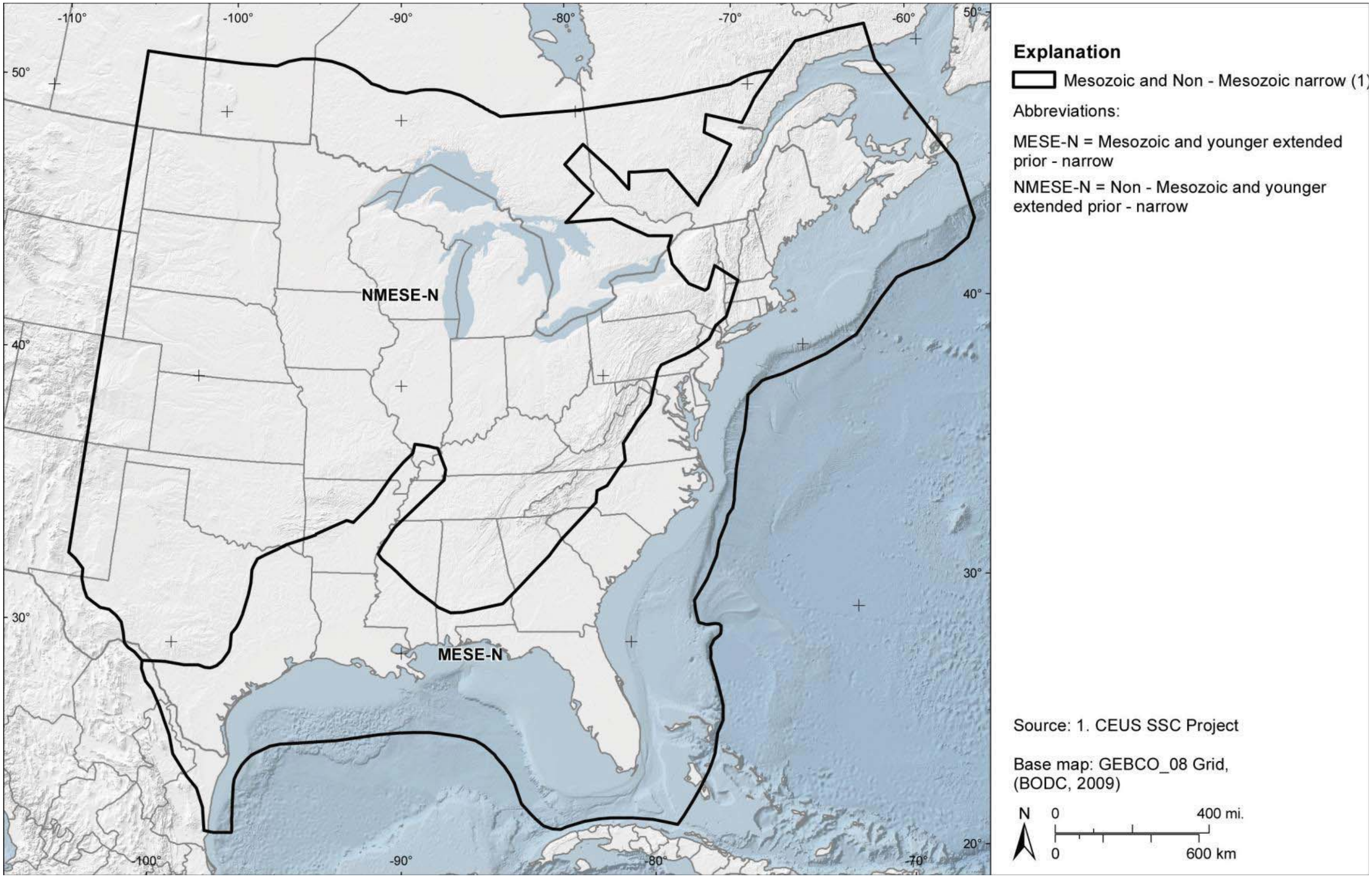

Figure H-3-3
Mesozoic extended (MESE-N) and non-extended (NMESE-N) Mmax zones for the "narrow" interpretation

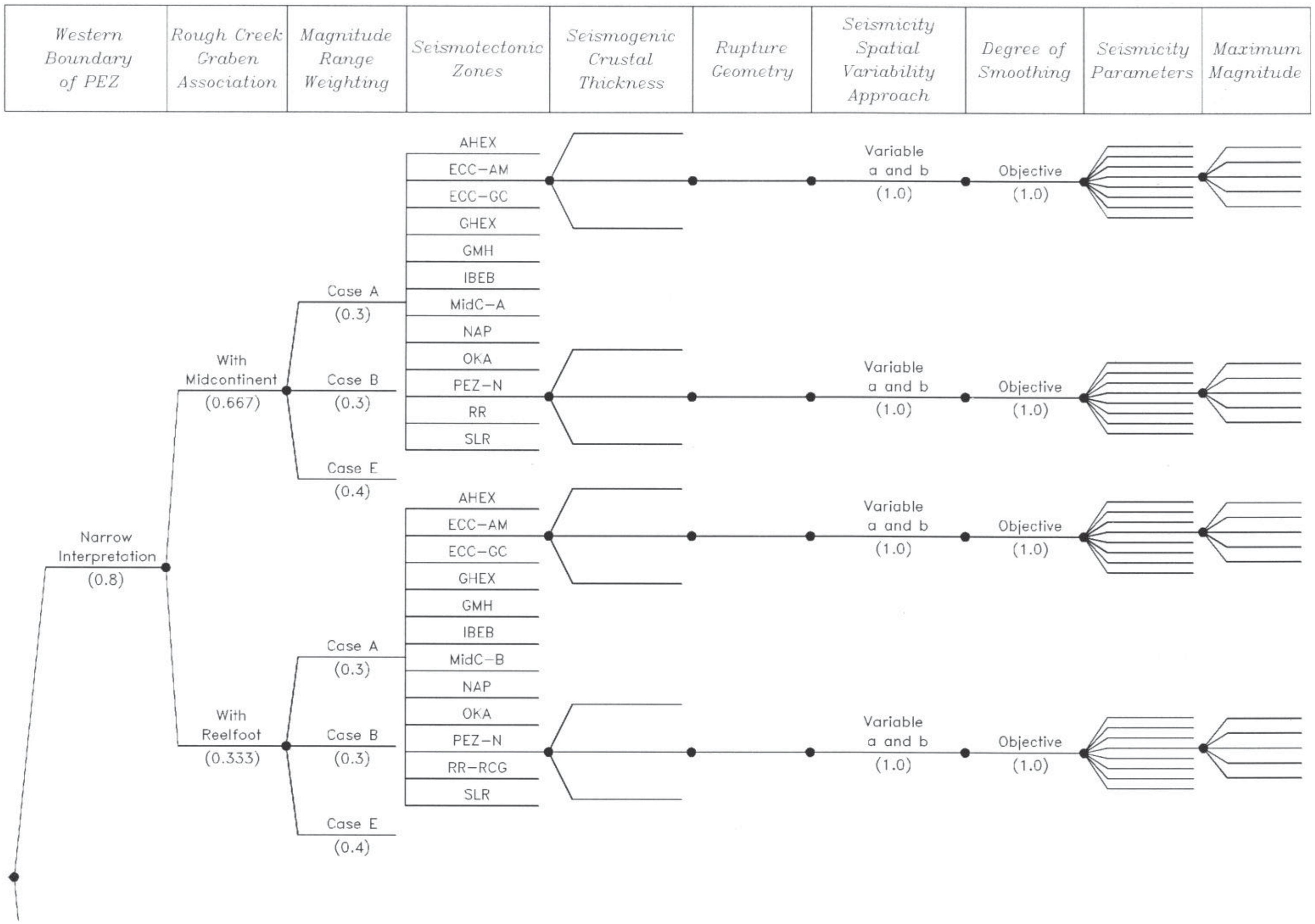

Figure H-4-1(a)
Logic tree for the seismotectonic zones branch of the master logic tree

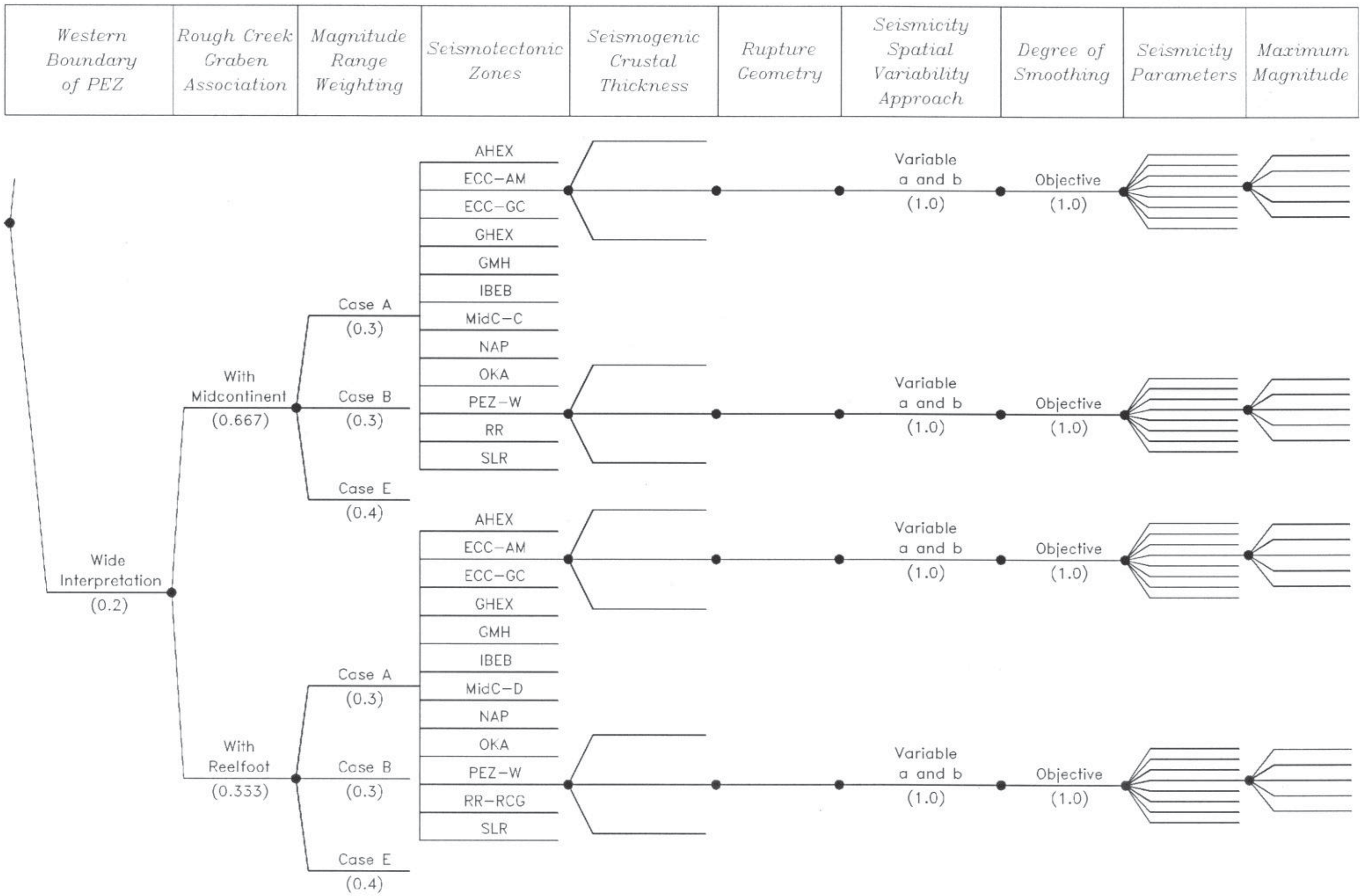

Figure H-4-1(b)
Logic tree for the seismotectonic zones branch of the master logic tree

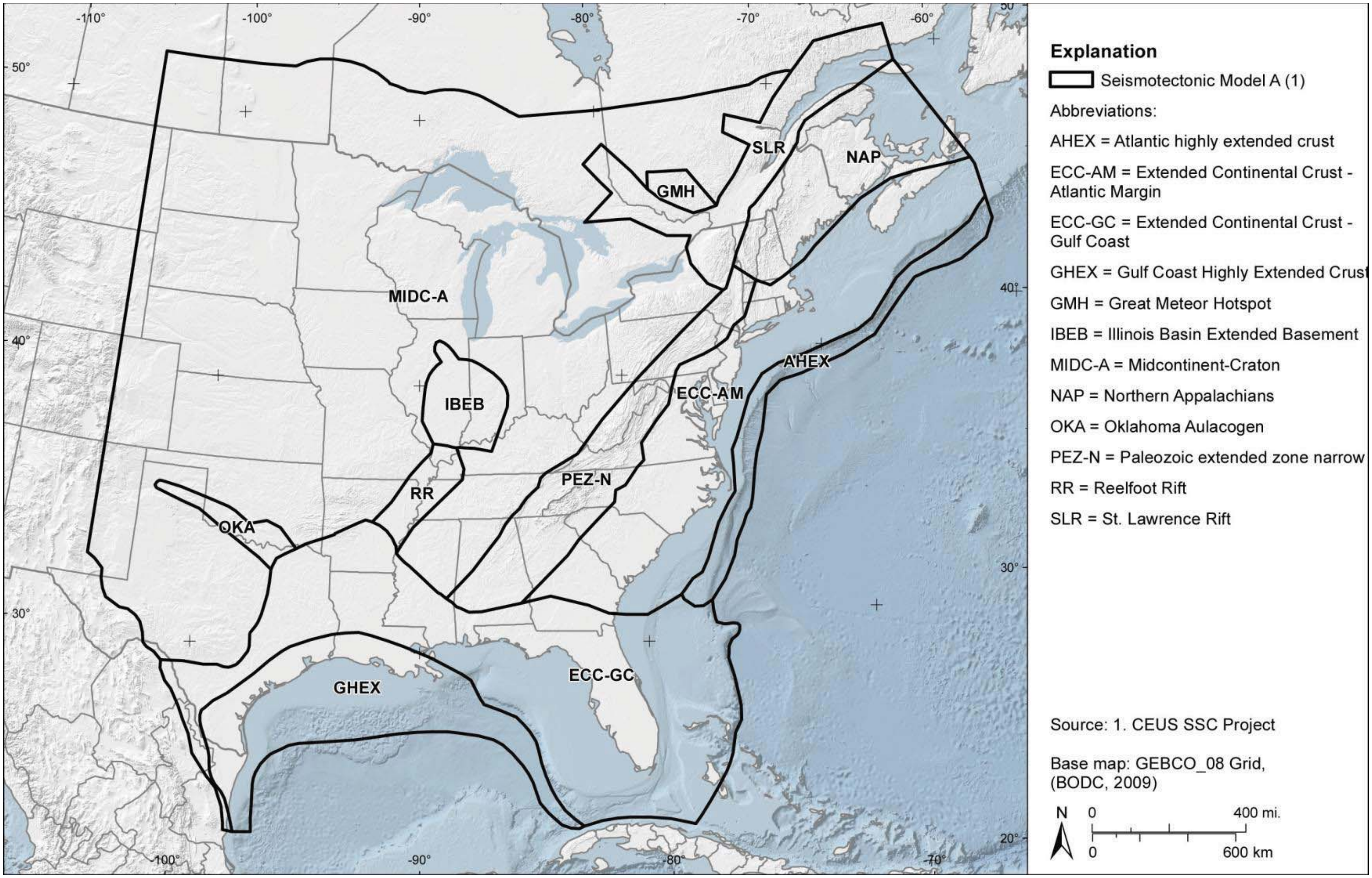

Figure H-4-2
Seismotectonic zones shown in the case where the Rough Creek Graben is not part of the Reelfoot Rift (RR) and the Paleozoic Extended zone is narrow (PEZ-N)

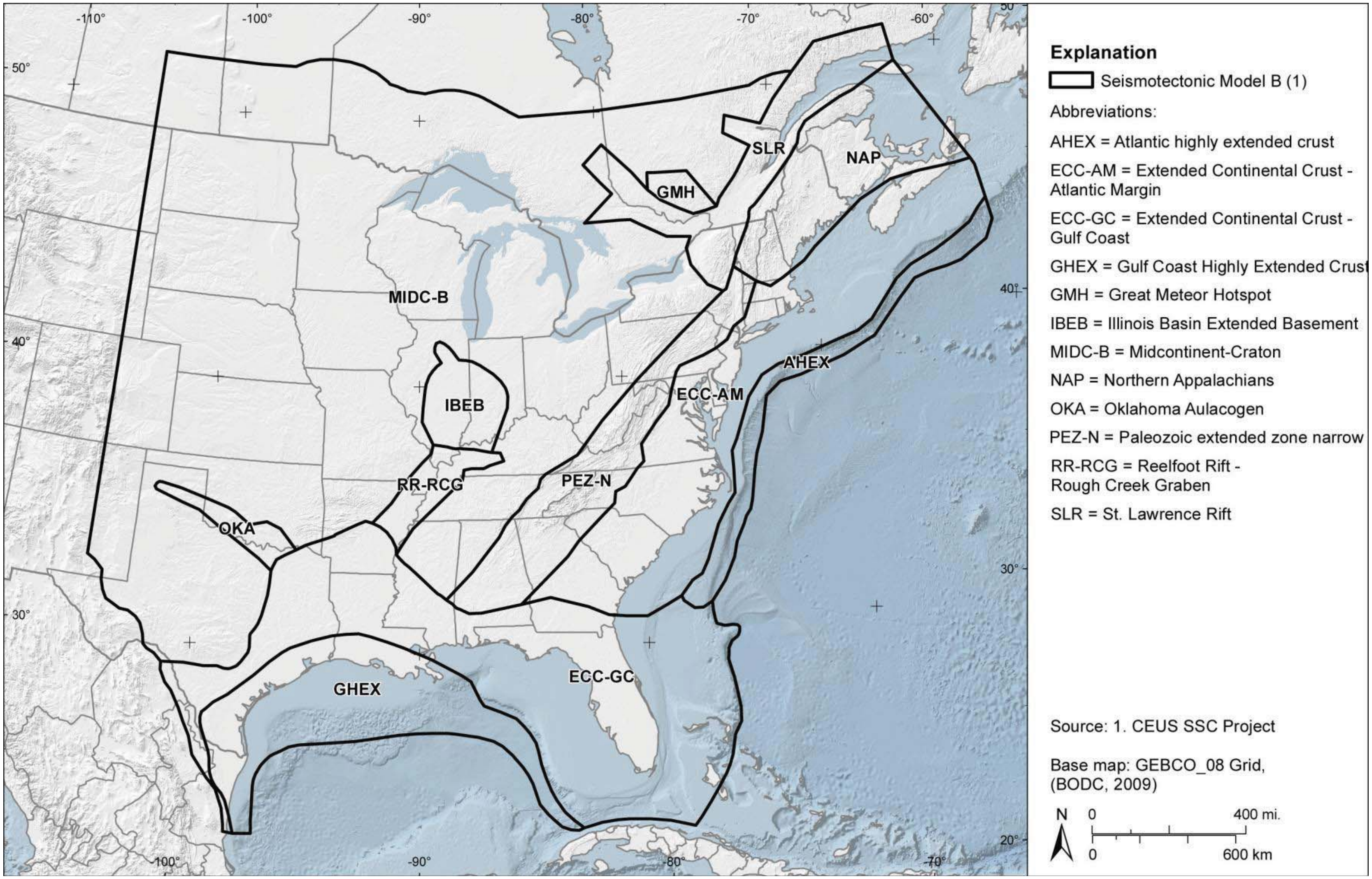

Figure H-4-3
Seismotectonic zones shown in the case where the Rough Creek Graben is part of the Reelfoot Rift (RR-RCG) and the Paleozoic Extended zone is narrow (PEZ-N)

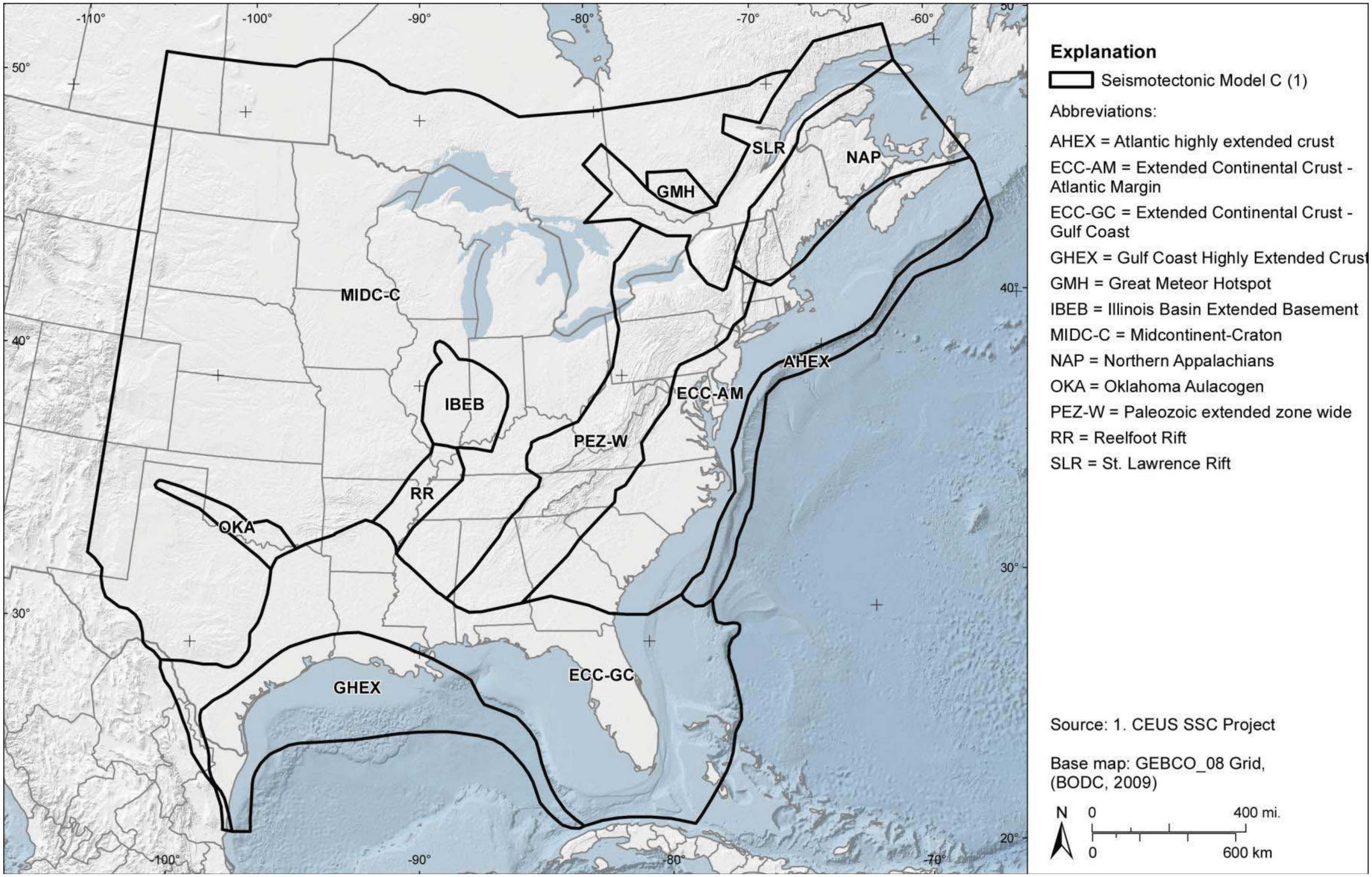

Figure H-4-4
Seismotectonic zones shown in the case where the Rough Creek Graben is not part of the Reelfoot Rift (RR) and the Paleozoic Extended zone is wide (PEZ-W)

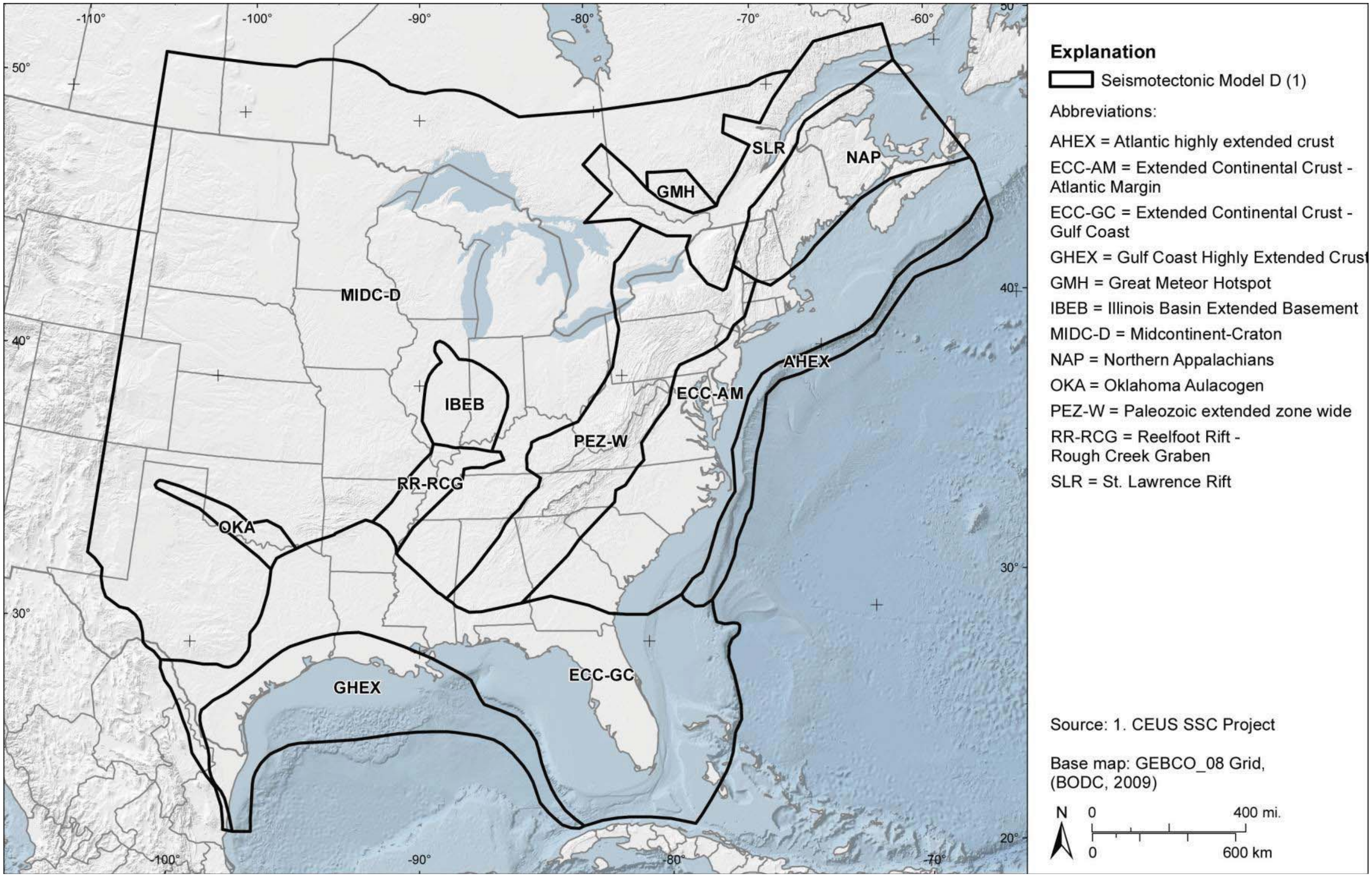

Figure H-4-5
Seismotectonic zones shown in the case where the Rough Creek Graben is part of the Reelfoot Rift (RR-RCG) and the Paleozoic Extended zone is wide (PEZ-W)

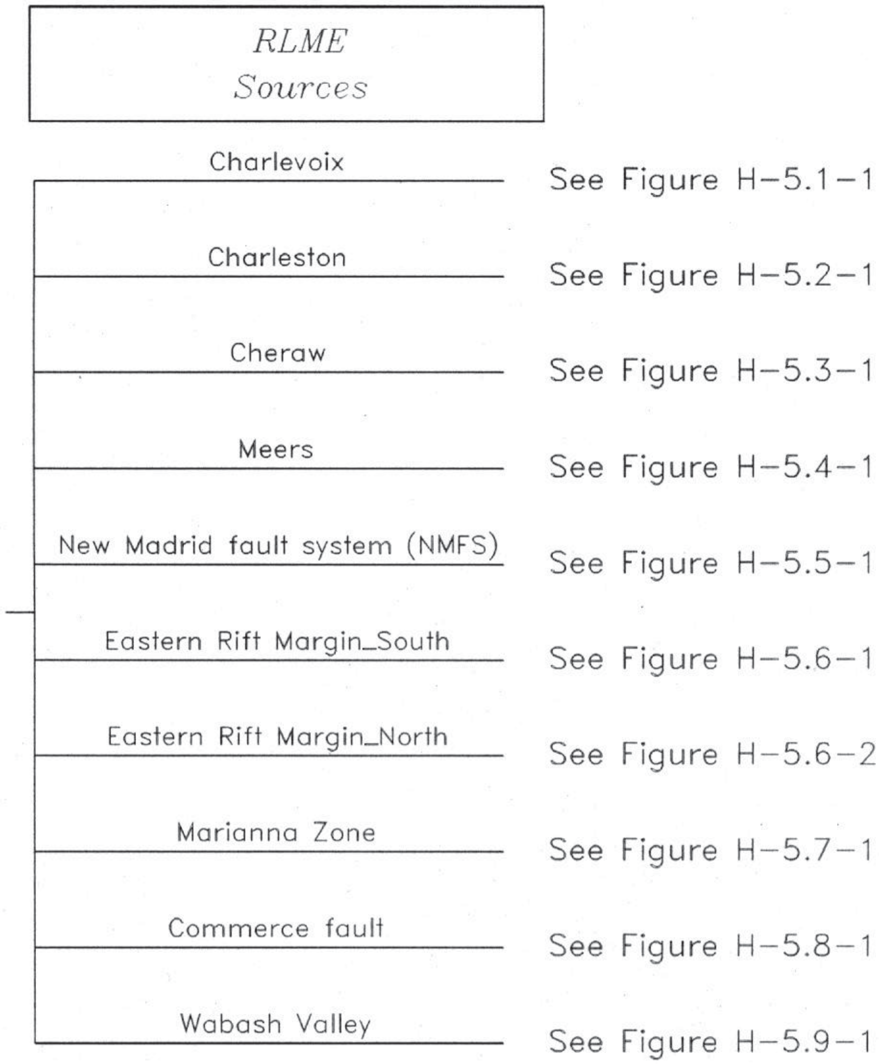

Figure H-5-1
Logic tree for the RLME source branch of the master logic tree

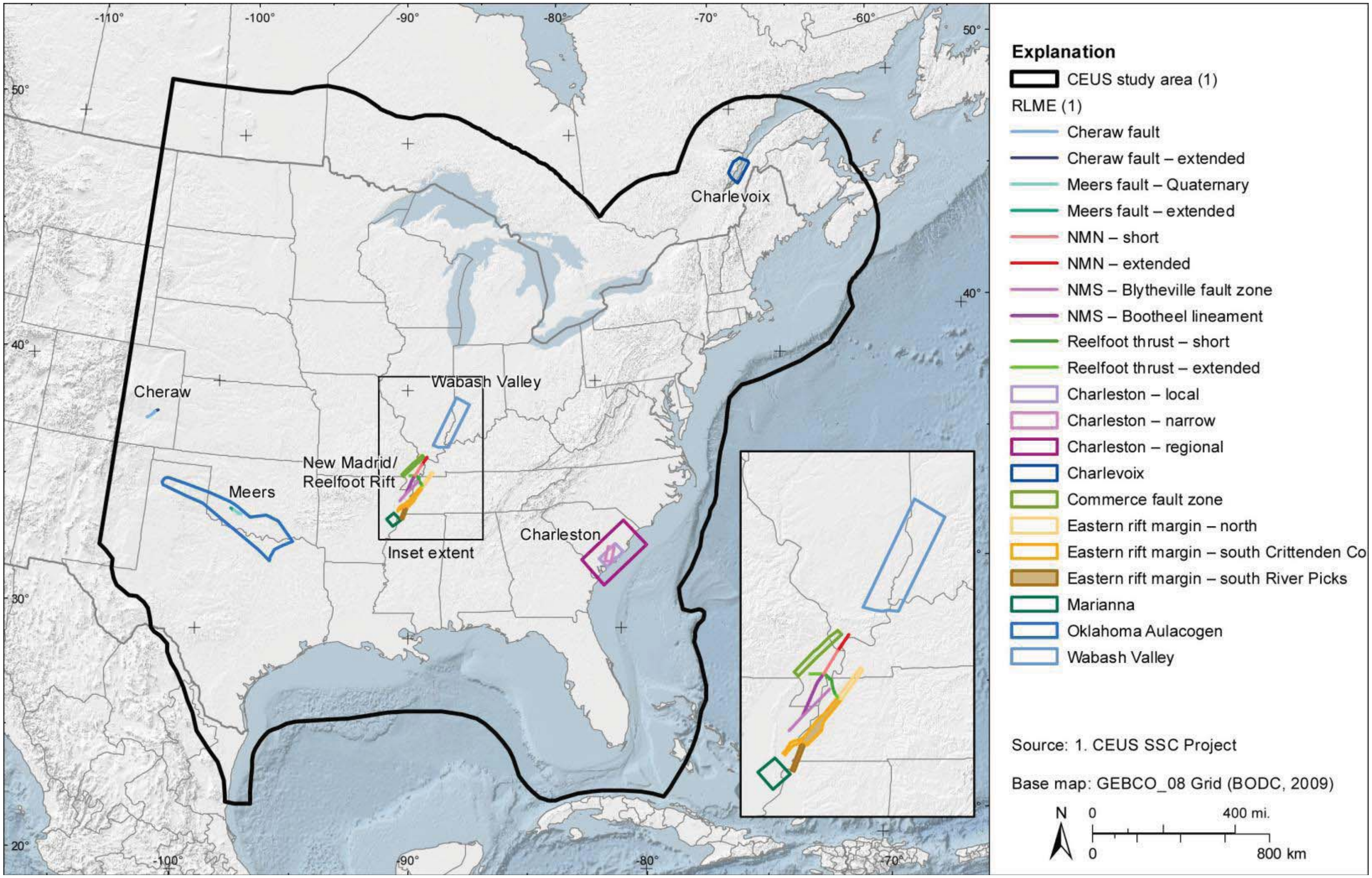

Figure H-5-2
Location of RLME sources in the CEUS SSC model

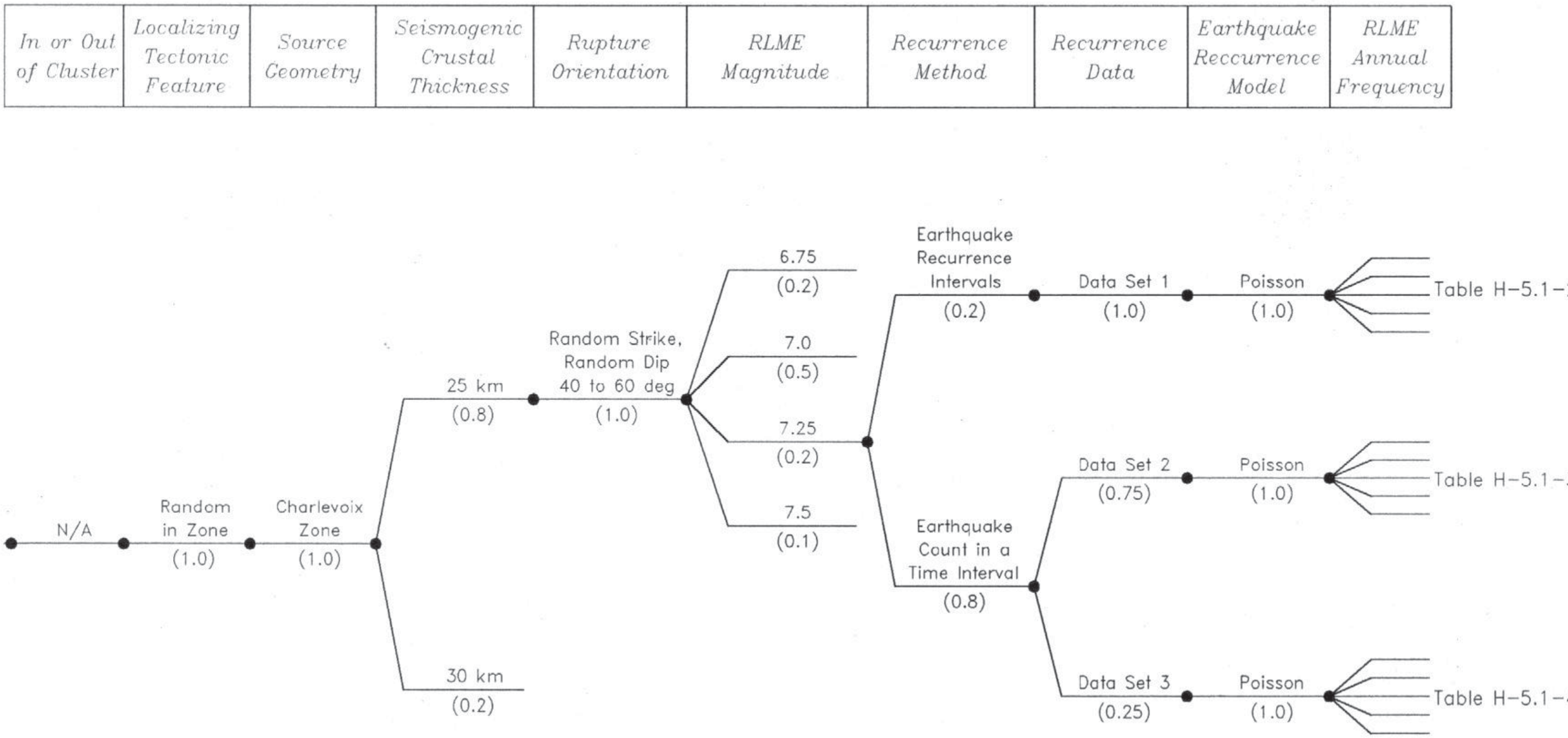

Figure H-5.1-1
Logic tree for Charlevoix RLME source

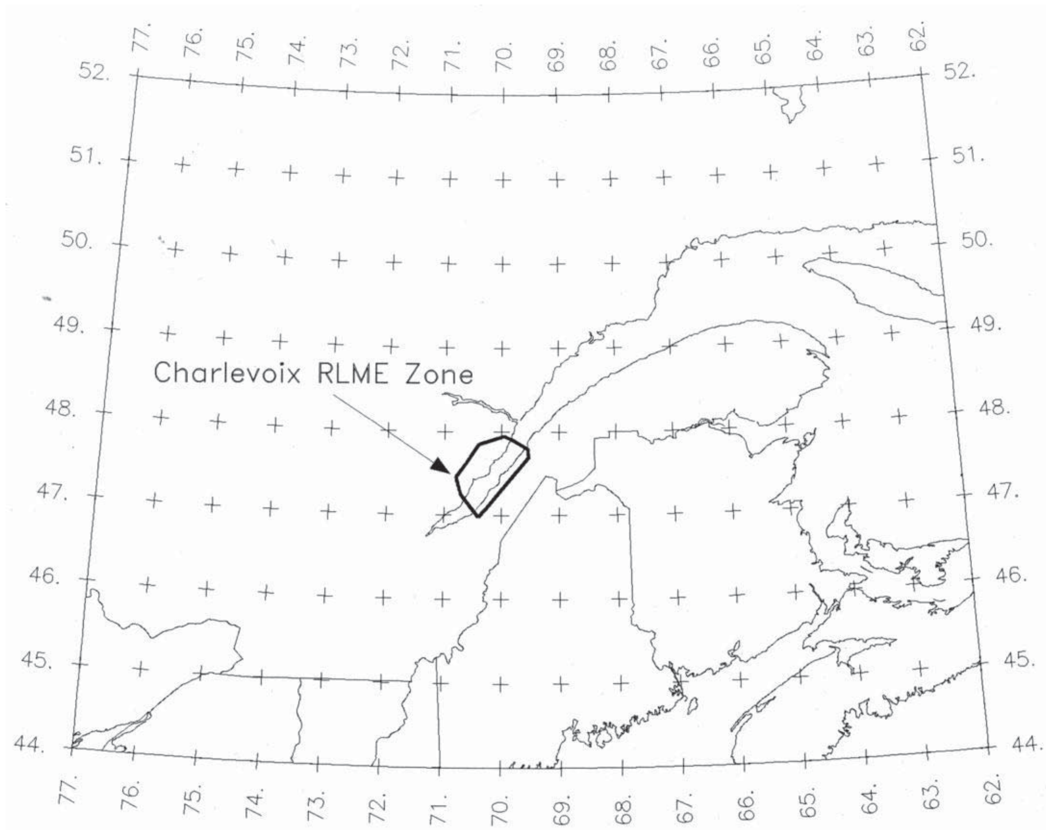

Figure H-5.1-2
Charlevoix RLME source geometry

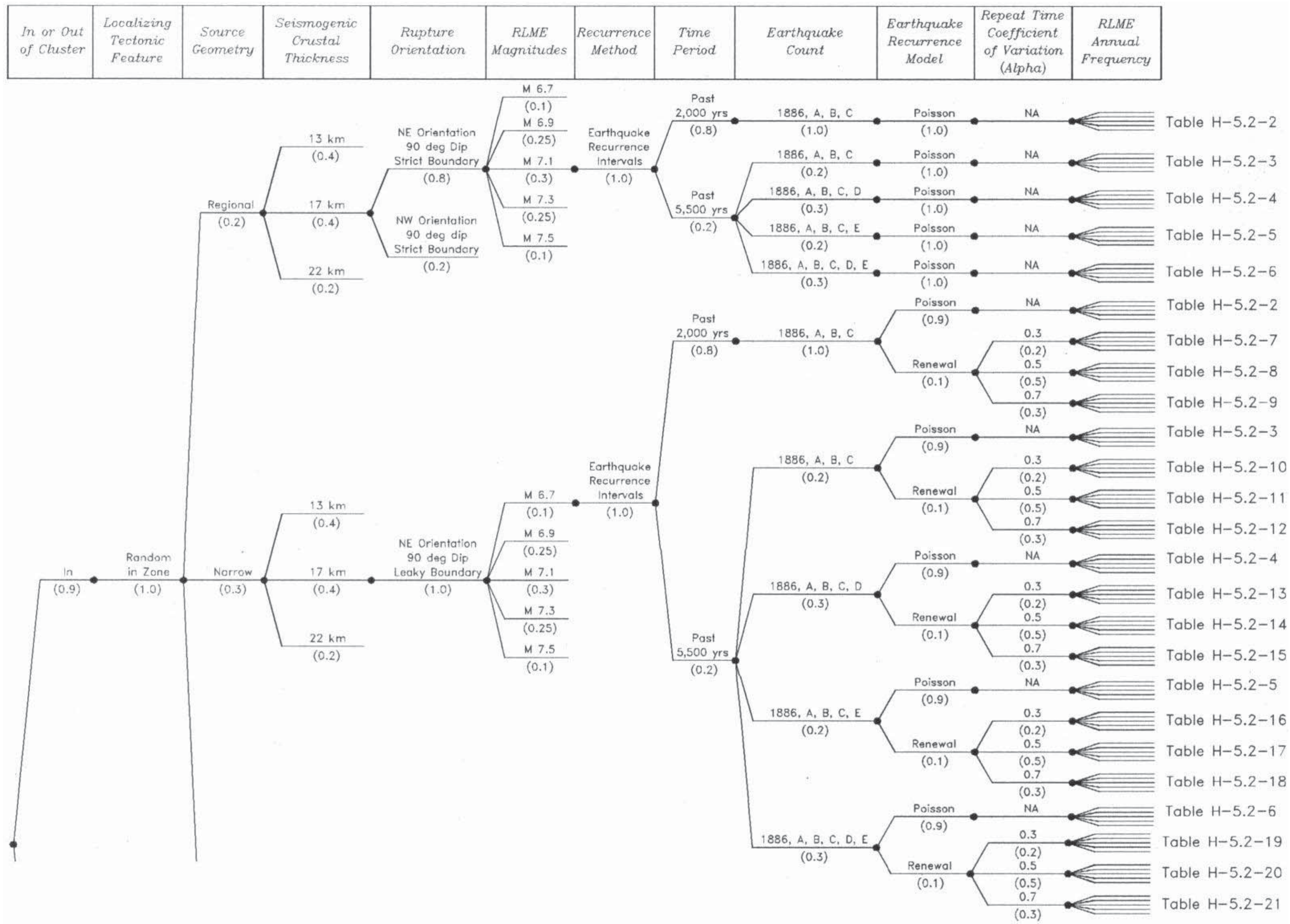

Figure H-5.2-1(a)
Logic tree for Charleston RLME source

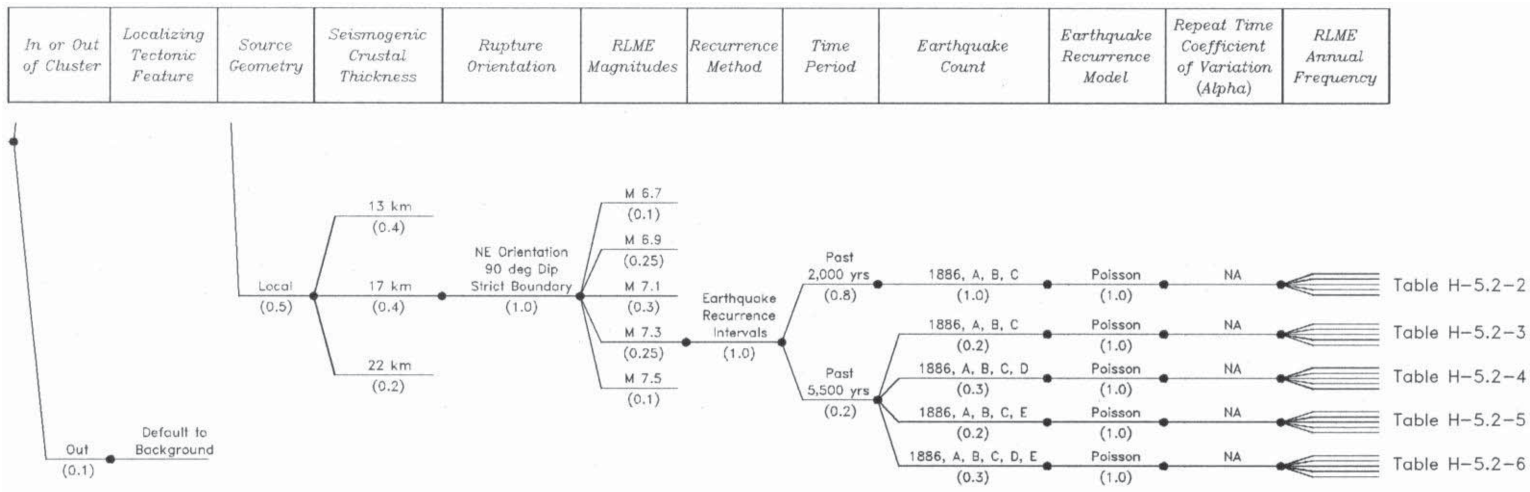

Figure H-5.2-1(b)
Logic tree for Charleston RLME source

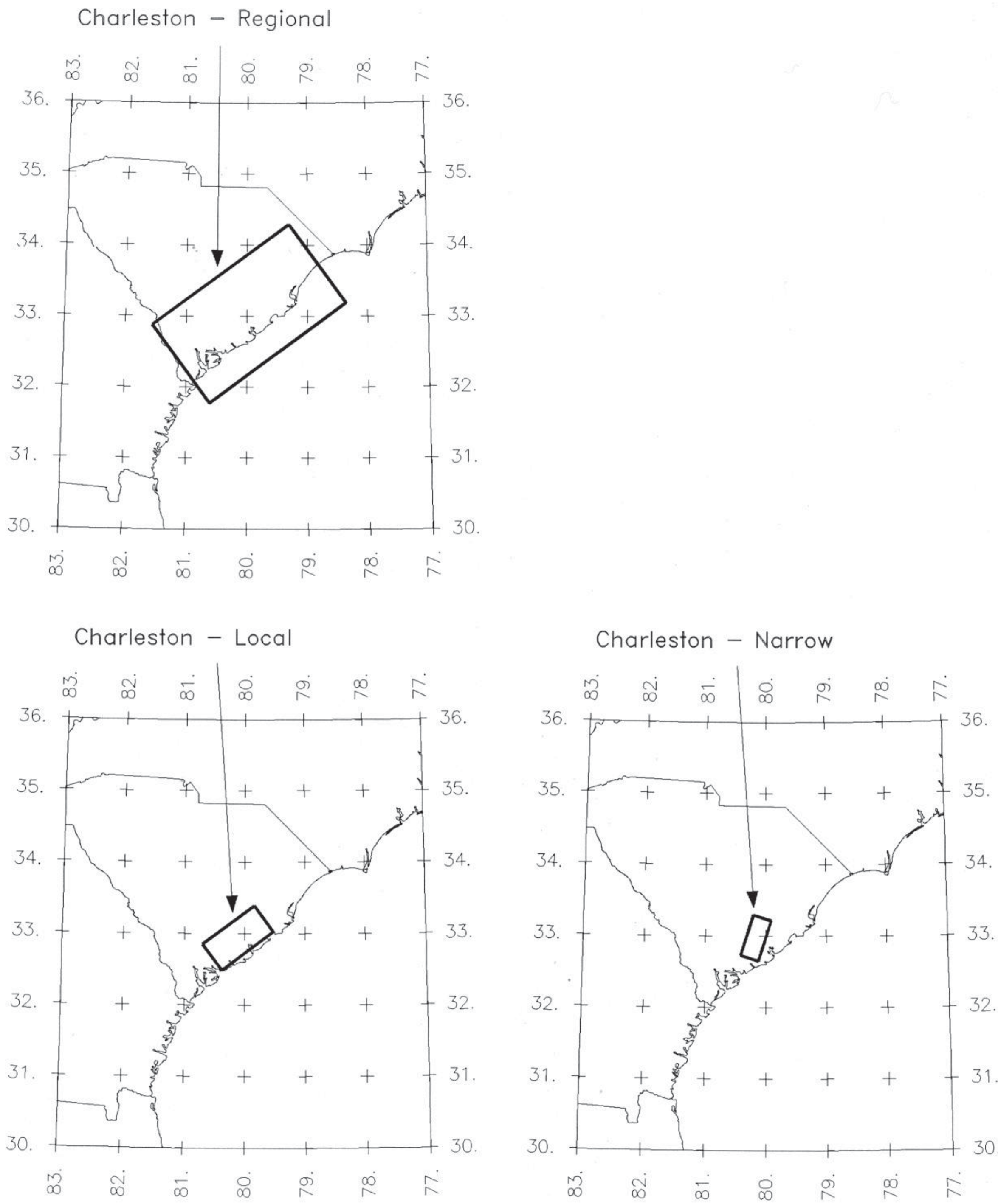

Figure H-5.2-2
Charleston RLME alternative source geometries

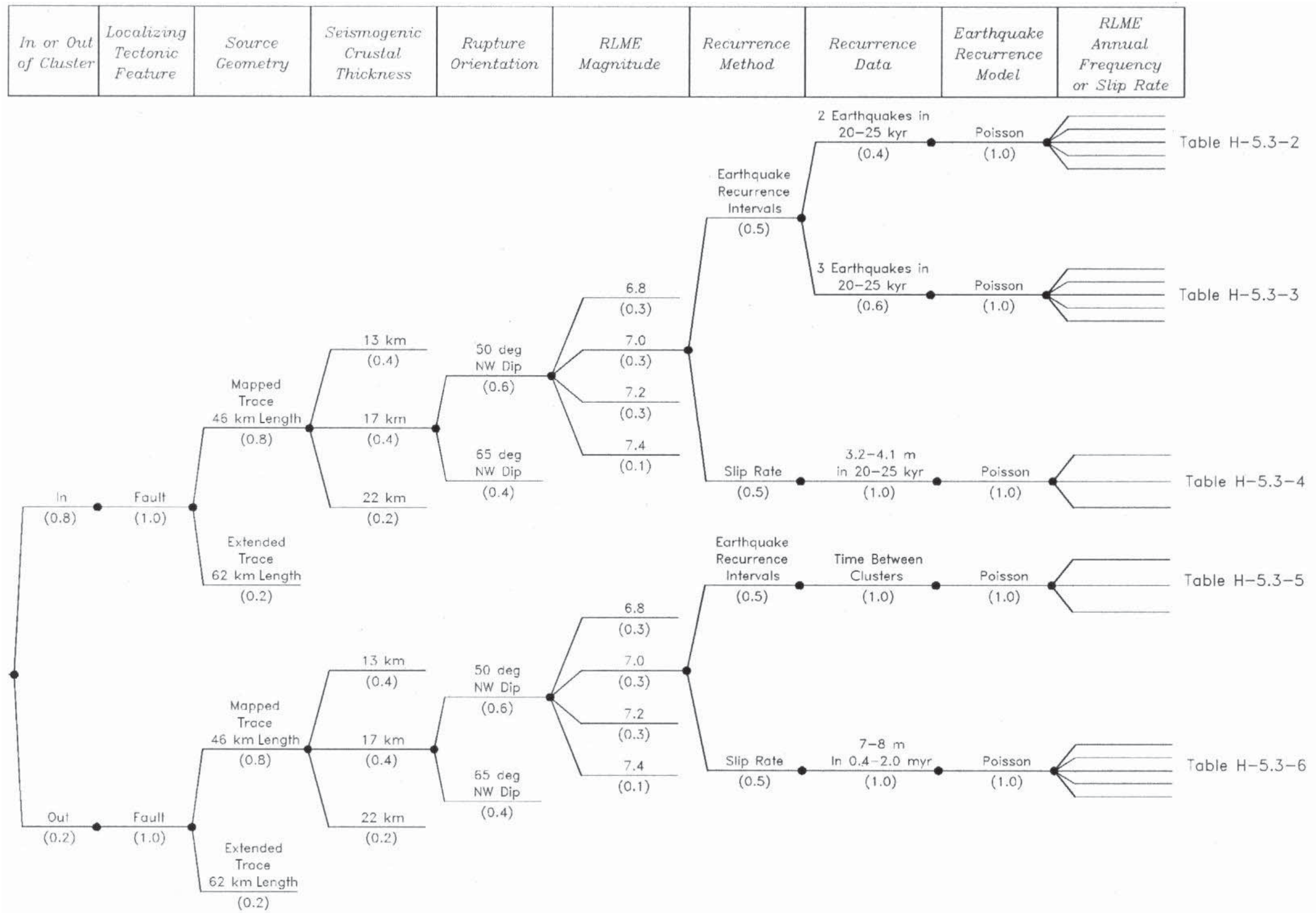

Figure H-5.3-1
Logic tree for Cheraw RLME source

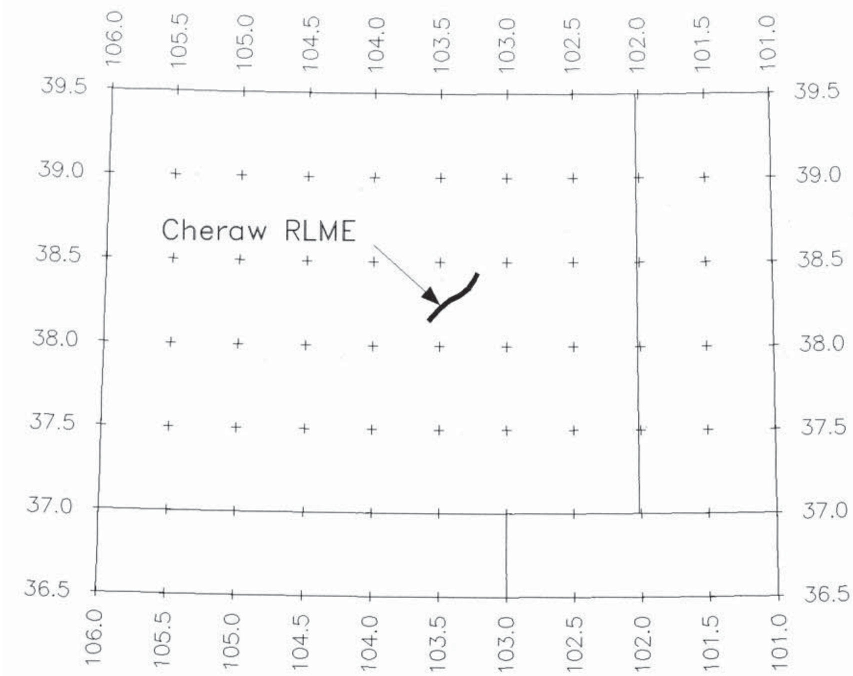

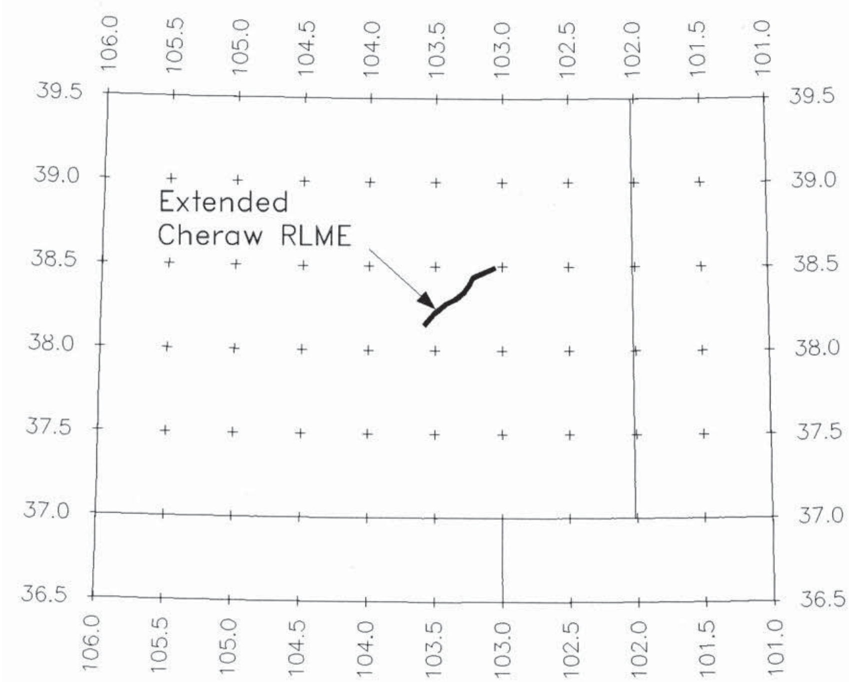

Figure H-5.3-2
Cheraw RLME source geometry

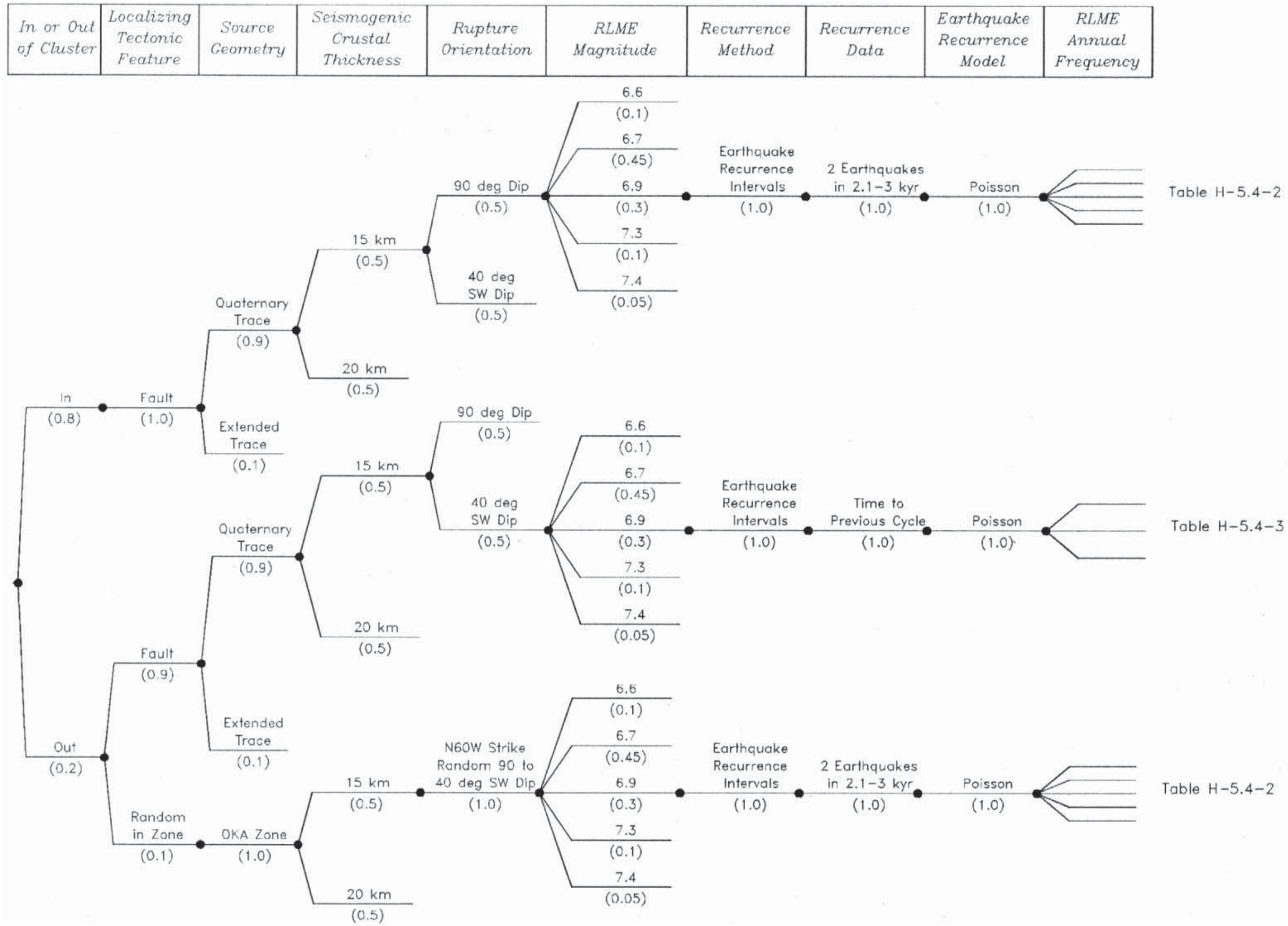

Figure H-5.4-1
Logic tree for Meers RLME source

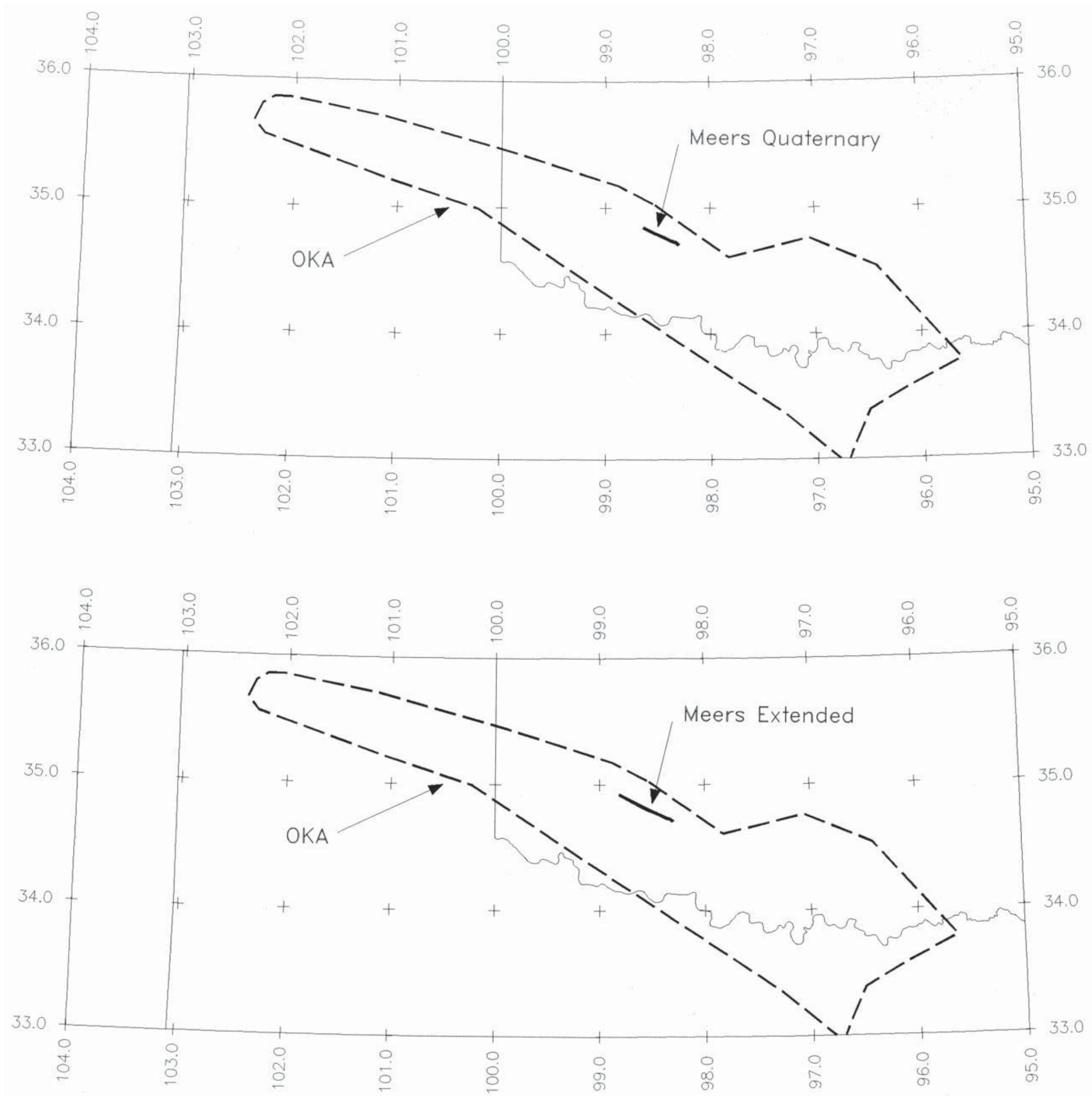

Figure H-5.4-2
Meers RLME source geometries

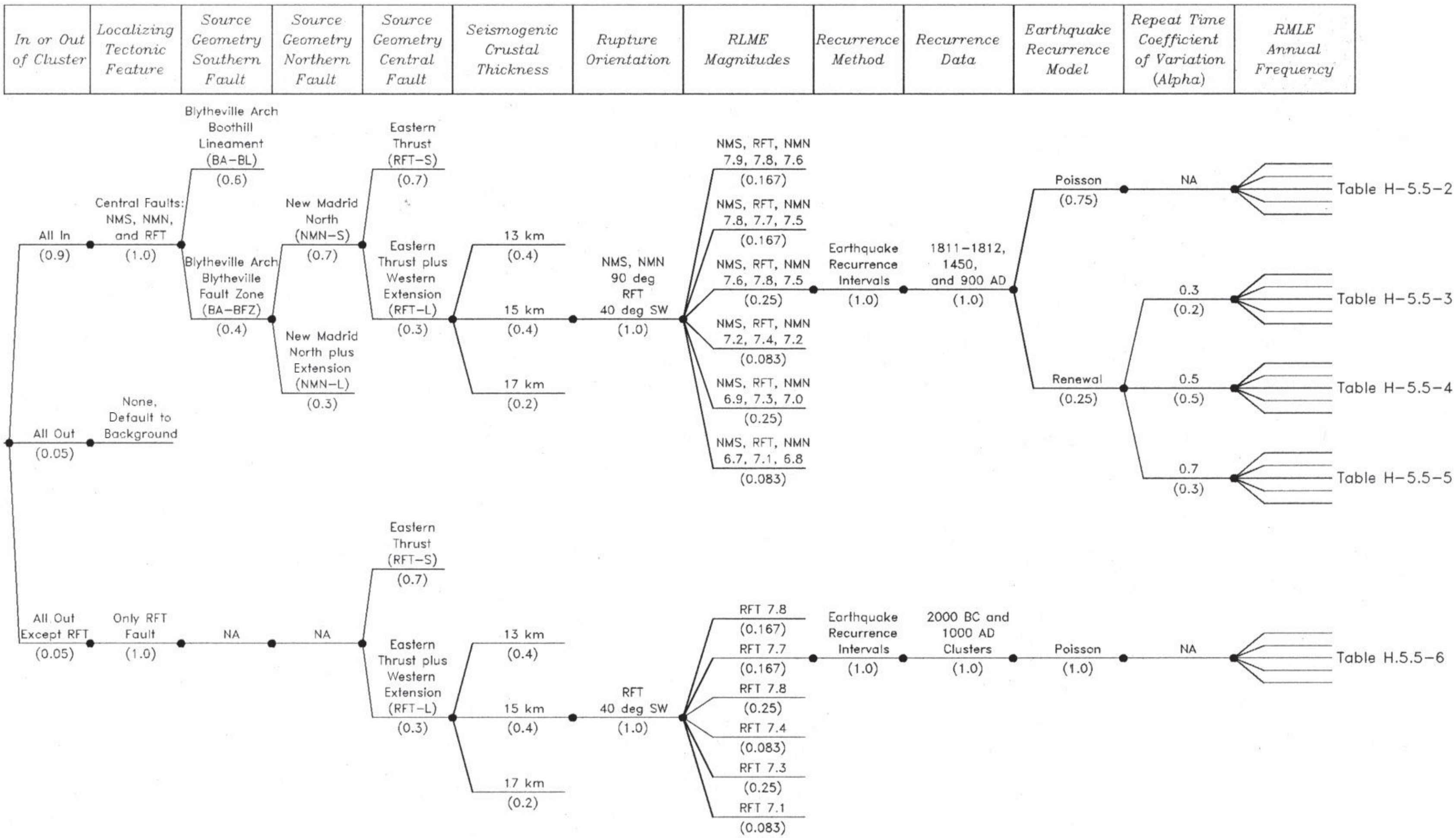

Figure H-5.5-1
Logic tree for NMFS RLME source

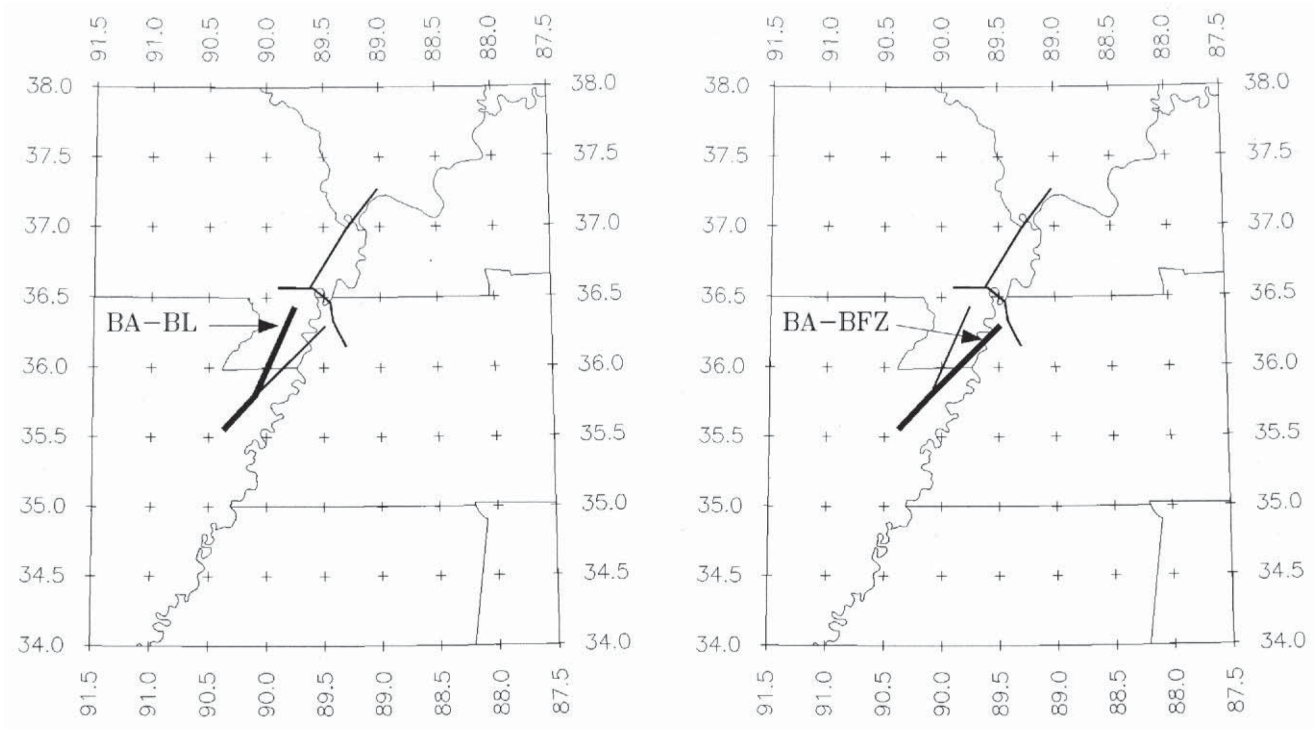

Figure H-5.5-2
New Madrid South (NMS) fault alternative RMLE source geometries: Blytheville Arch-Bootheel Lineament (BA-BL) and Blytheville Arch-Blytheville fault zone (BA-BFZ)

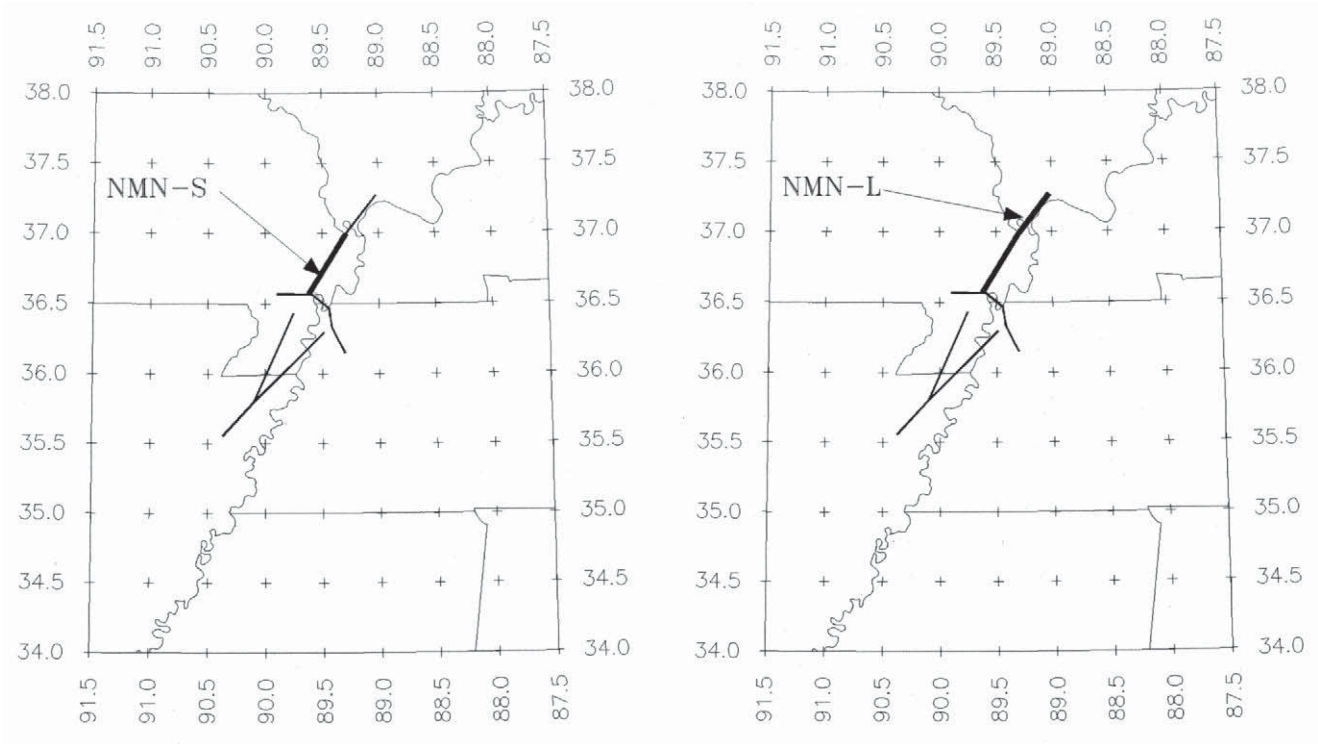

Figure H-5.5-3
New Madrid North (NMN) fault alternative RMLE source geometries: New Madrid North (NMN_S) and New Madrid North plus extension (NMN_L)

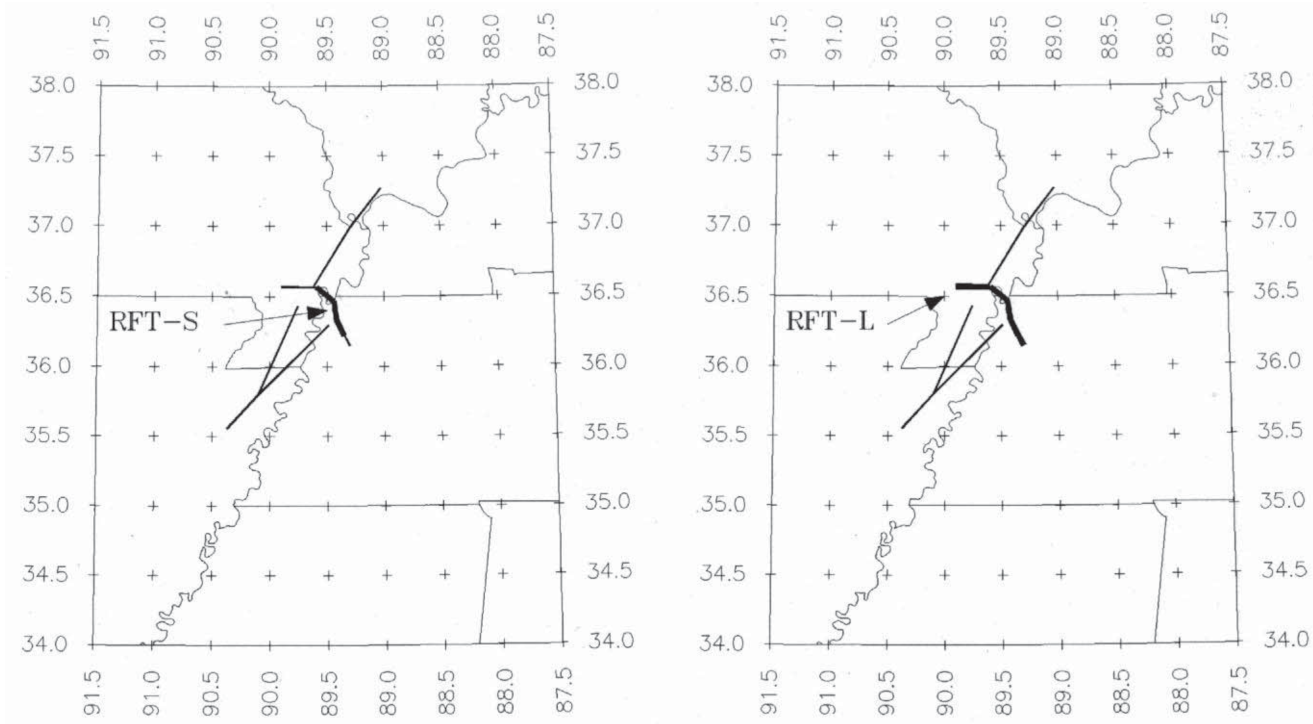

Figure H-5.5-4
Reelfoot Thrust (RFT) fault alternative RMLE source geometries: Reelfoot thrust (RFT_S) and Reelfoot thrust plus extensions (RFT_L)

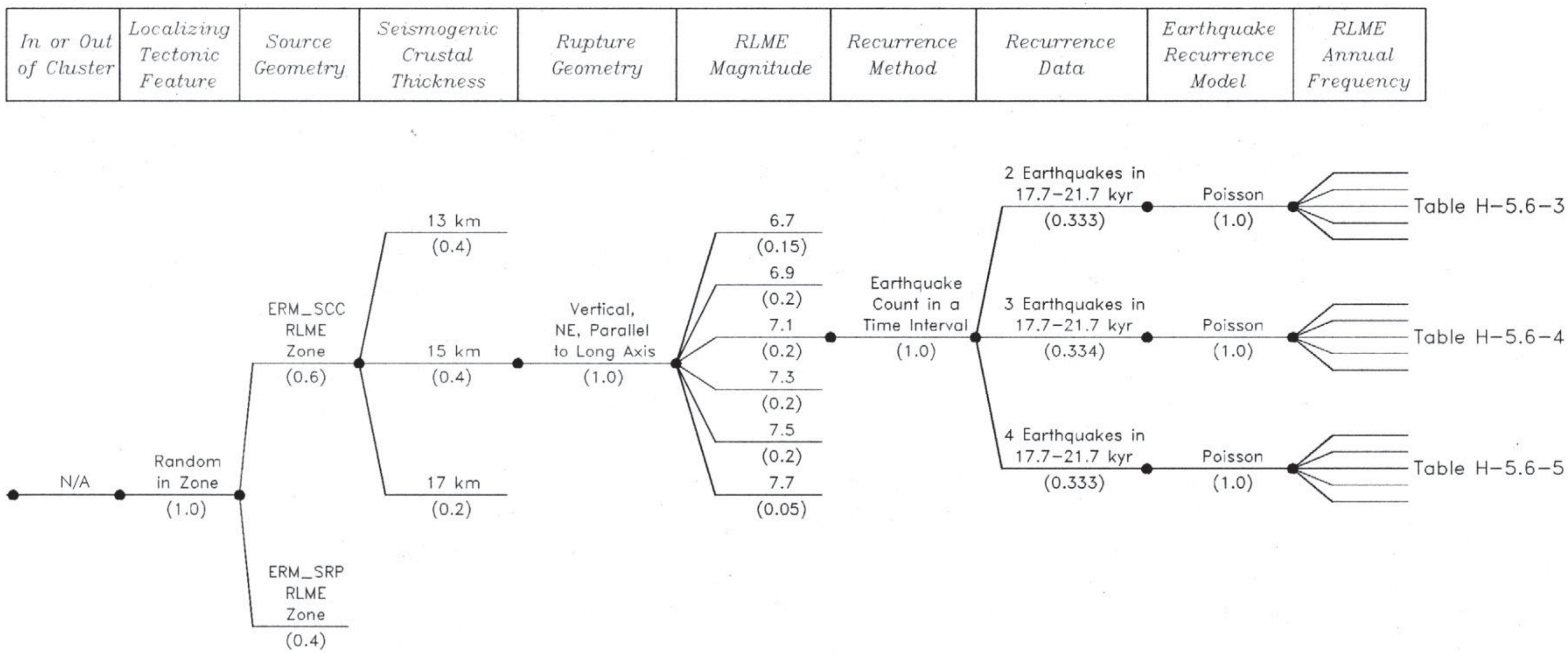

Figure H-5.6-1
Logic tree for ERM-S RLME source

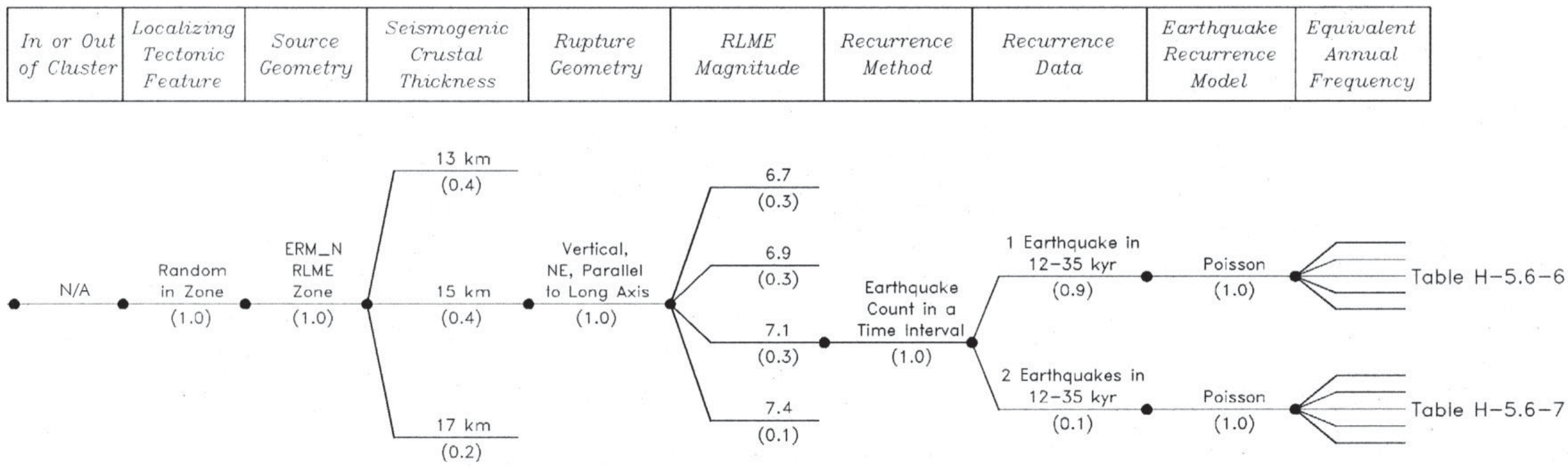

Figure H-5.6-2
Logic tree for ERM-N RLME source

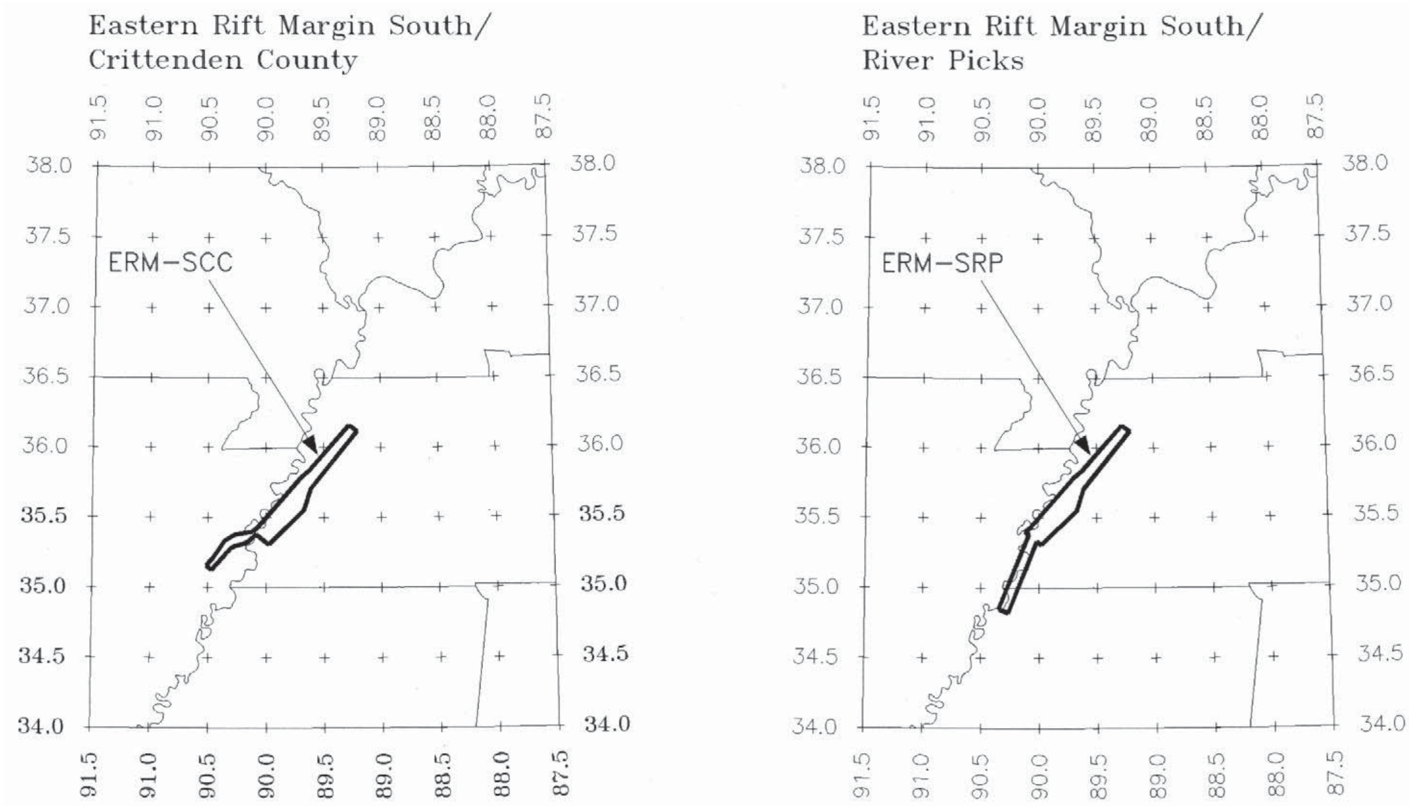

Figure H-5.6-3
ERM-S RLME source geometries

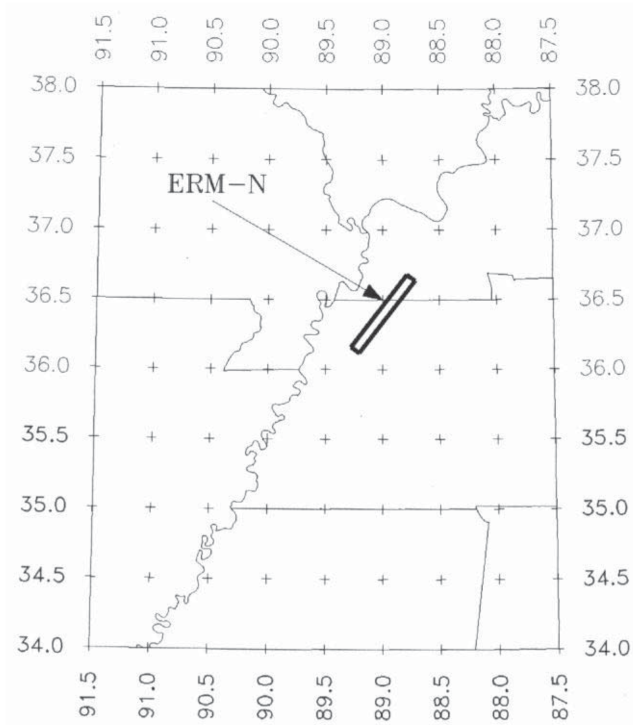

Figure H-5.6-4
ERM-N RLME source geometry

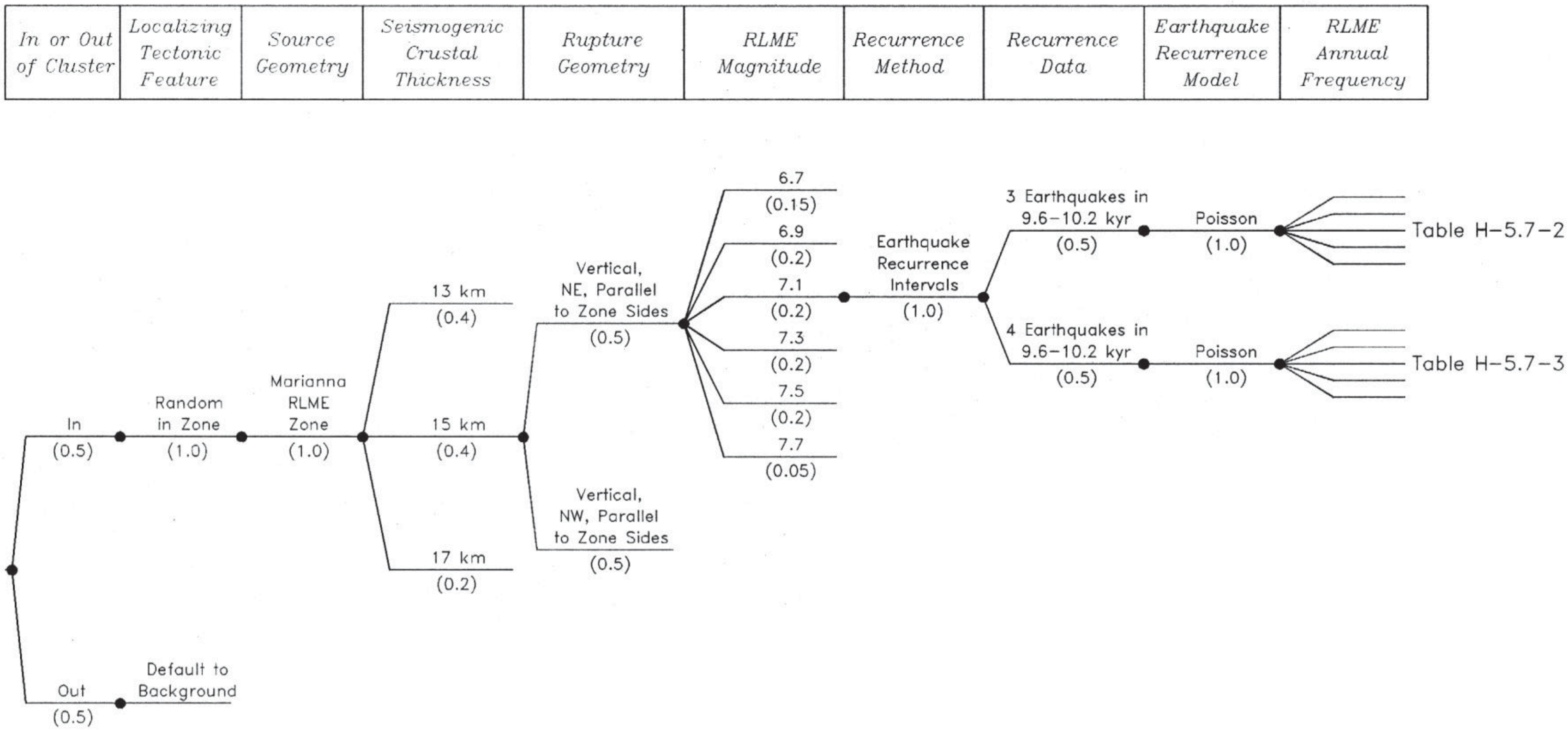

Figure H-5.7-1
Logic tree for Marianna RLME source

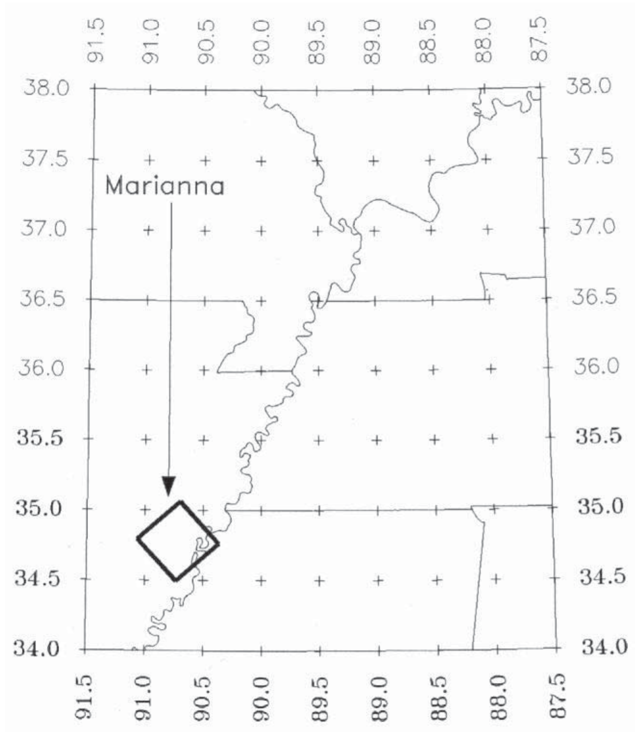

Figure H-5.7-2
Marianna RLME source geometry

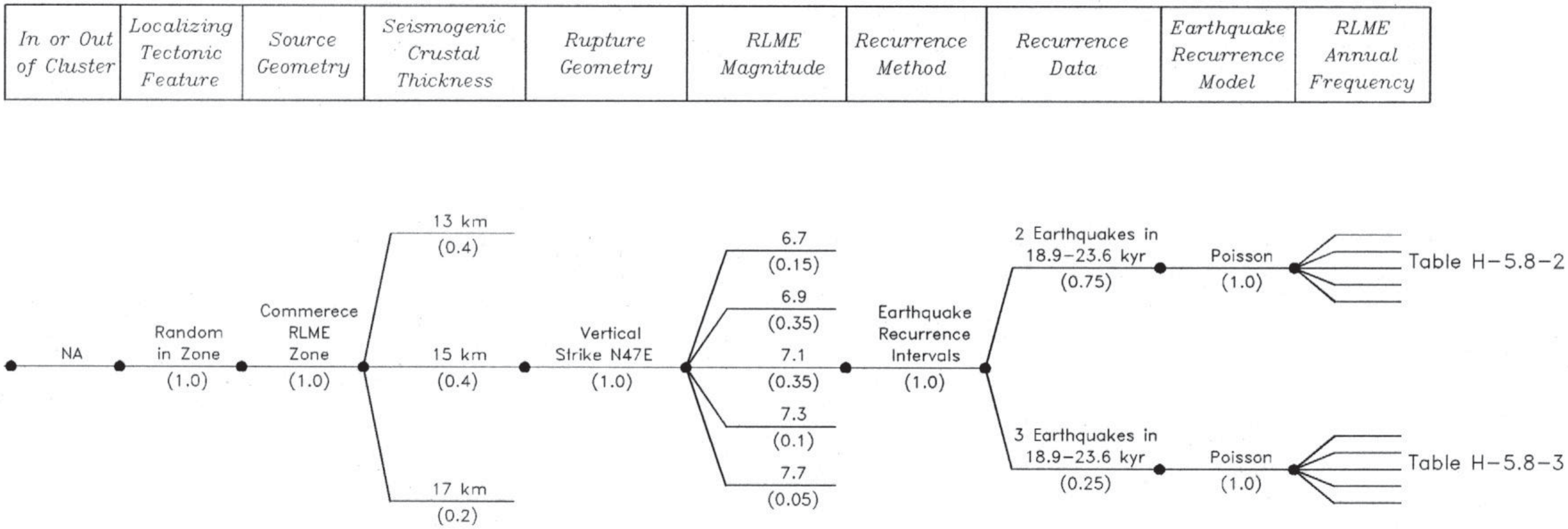

Figure H-5.8-1
Logic tree for Commerce Fault Zone RLME source

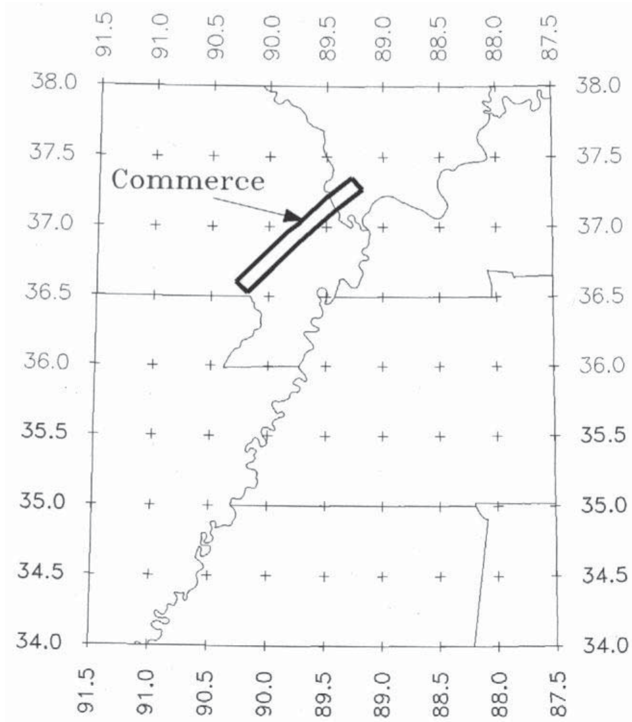

Figure H-5.8-2
Commerce RLME source geometry

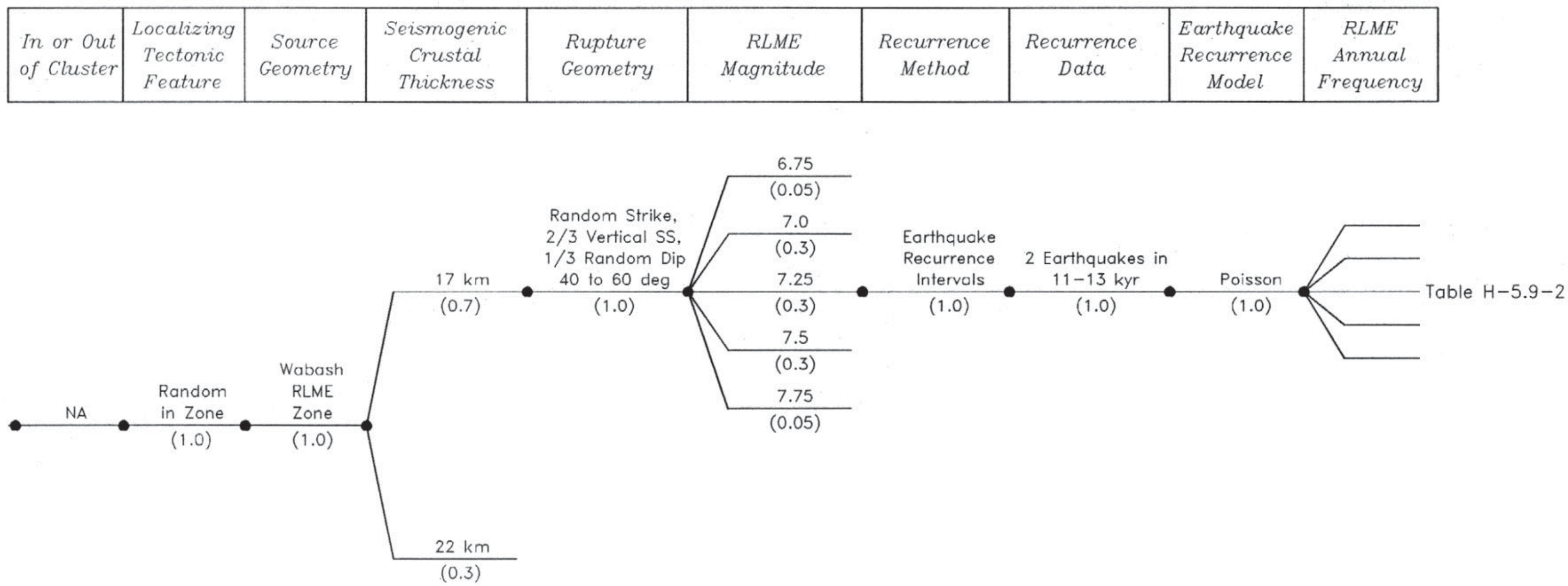

Figure H-5.9-1
Logic tree for Wabash Valley RLME source

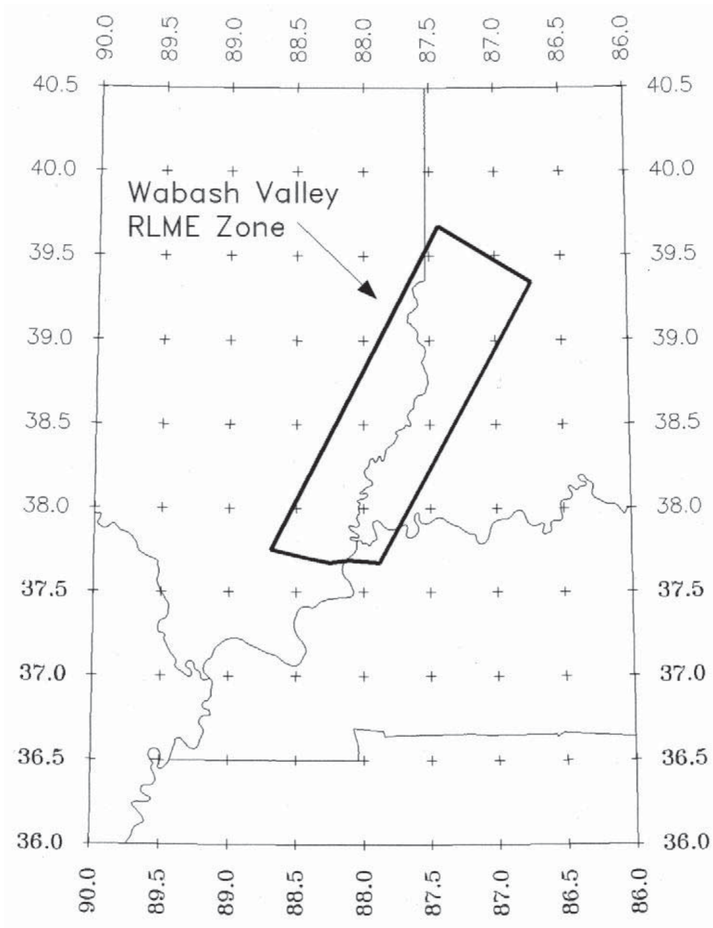

Figure H-5.9-2
Wabash Valley RLME source geometry